An Open Publishing Platform of the Organization for Human Brain Mapping
APERTURE NEURO

ORIGINAL RESEARCH ARTICLE

Quantitative streamlines tractography: methods and inter-subject normalisation

Robert E. Smith[a,b], David Raffelt[a], J-Donald Tournier[c], Alan Connelly[a,b,d]

[a] *The Florey Institute of Neuroscience and Mental Health, Heidelberg, Victoria, Australia*
[b] *Florey Department of Neuroscience and Mental Health, University of Melbourne, Melbourne, Victoria, Australia*
[c] *Centre for the Developing Brain, School of Biomedical Engineering & Imaging Sciences, King's College London, London, UK*
[d] *Department of Medicine, Austin Health and Northern Health, University of Melbourne, Melbourne, Victoria, Australia*

ABSTRACT

Recent developments in semi-global tractogram optimisation algorithms have opened the field of diffusion magnetic resonance imaging (MRI) to the possibility of performing *quantitative* assessment of structural fibre 'connectivity'. The proper application of these methods in neuroscience research has, however, been limited by a lack of awareness, understanding, or appreciation for the consequences of these methods; furthermore, particular steps necessary to use these tools in an appropriate manner to fully exploit their quantitative properties have not yet been described. This article therefore serves three purposes: to increase awareness of the fact that there are *existing tools* that attempt to address the well-known non-quantitative nature of streamlines counts; to illustrate *why* these algorithms work the way they do to yield quantitative estimates of white matter 'connectivity' (in the form of total intra-axonal cross-sectional area: 'fibre bundle capacity (FBC)'); and to explain how to properly utilise these results for quantitative tractography analysis *across subjects*.

Keywords: Magnetic resonance imaging, diffusion, white matter, streamlines tractography, quantification

Corresponding author: Robert E Smith, Florey Institute of Neuroscience and Mental Health, Melbourne Brain Centre, 245 Burgundy Street, Heidelberg, Victoria 3084, Australia, Phone: (+61 3) 9035 7128, Fax: (+61 3) 9035 7301, Email: robert.smith@florey.edu.au

Received: 02.10.2020

Accepted: 24.01.2022

DOI: 10.52294/ApertureNeuro.2022.2.NEOD9565

ABBREVIATIONS

AFD: apparent fibre density;
COMMIT: convex optimisation modelling for microstructure-informed tractography;
DWI: diffusion-weighted imaging (/image)
FBA: fixel-based analysis;
FBC: fibre bundle capacity (an estimate of the bandwidth of a white matter pathway);
FC: fibre cross-section (NB: macroscopic change in);
FD: fibre density (microscopic);
FDC: fibre density and cross-section (combined measure of FD and FC);
'fixel': specific *fi*bre population within a vox*el*;
FOD: fibre orientation distribution;
LiFE: linear fascicle evaluation;
SIFT: spherical-deconvolution informed filtering of tractograms.

INTRODUCTION

Since the introduction of tractography to the field of diffusion magnetic resonance imaging (MRI), there has been extensive interest in the use of this technology to assess fibre 'connectivity' in the brain for various neuroscientific applications.[1–4] The vast majority of tractography algorithms operate on the same fundamental mechanism: the 'streamlines' algorithm, where plausible white matter fibre pathways are constructed by iteratively propagating along the local estimated fibre orientation.[5–9] Unfortunately, this mechanism of reconstruction does not directly facilitate

one of the most fundamental parameters of interest: the *density* of 'connectivity' between two brain regions.[10] A major contributing factor to this limitation is that while the streamlines algorithm enforces that the reconstructed trajectories obey the estimated *orientations* of the underlying fibre bundles, it provides no meaningful control over the reconstructed *densities* of those bundles.

The class of 'global tractography' methods[11–15] has for many years shown promise to circumvent this problem. While in the 'streamlines' algorithm individual white matter trajectories are propagated independently and using only local fibre orientation information, these 'global' methods simultaneously solve for all connections at once, in a manner that enforces the entire tractogram reconstruction to be consistent with the raw diffusion image data. Even the most modern of these methods, however, incur considerable computational expense (particularly as reconstructions with greater numbers of connections are sought), and typically do not provide any guarantees regarding the construction of connections with biologically meaningful terminations, for instance, resulting in terminations in the white matter or cerebrospinal fluid (CSF) that are otherwise considered erroneous.[16,17]

A new class of 'semi-global' tractogram optimisation algorithms offers a potential compromise[18–22]; these have additionally been referred to as 'tractogram filtering', 'microstructure-informed tractography', and 'top-down' algorithms in various contexts. These approaches take as input a whole-brain tractogram generated using one or more streamlines tractography algorithms and *modify* the reconstruction in some way such that the local streamlines densities become consistent with the density of underlying fibres evidenced by the image data. These methods therefore enable *quantitative* assessment of fibre 'connectivity' (within the myriad other associated limitations of diffusion MRI and streamlines tractography), with whole-brain reconstructions that are sufficiently dense to enable higher-level analyses (e.g. connectomics[23,24]) within reasonable computational requirements.

Despite the potential influence of these methods on the neuroimaging field, they have had only limited uptake. This may be due to a lack of awareness of the public availability of such methods, or a lack of understanding that these methods address some of the origins of the limitations of raw streamline count as a metric of 'connectivity'. Furthermore, although these methods seek to modulate the relative connection densities of different white matter pathways within a single brain, the appropriate mechanism by which these quantities should be compared *across subjects* has not yet been comprehensively explained in the literature. This article therefore serves three purposes, with the aim of increasing the utility of these tools in the field:

- *Alert* a wider audience to the fact that a primary contributing factor to the non-quantitative nature of streamlines counts can be addressed using freely available methods;
- Carefully explain and demonstrate *why* the design of these methods is appropriate to provide estimates of white matter connection density, including in the context of structural connectome construction;
- Explain *how* these estimates of connection density should be handled when performing *direct comparisons between subjects*.

BACKGROUND

Before addressing the major points of this article, we first clarify the specific position and role of these 'semi-global' tractography optimisation algorithms, the 'connectivity' metric of interest to be derived from them, and the limitations within which they operate.

Requisite knowledge

The specific 'semi-global' methods under discussion here are intrinsically dependent on both voxel-level modelling of diffusion MRI data and streamlines tractography. As such, an adequate understanding of those concepts will be necessary for readers to follow the logic presented here; these topics are covered extensively by prior publications.[2,5,9,10,25–33]

Context and role of semi-global algorithms

Figure 1 presents the role of these methods within a tractography-based reconstruction pipeline.

- Some biological white matter bundle of interest (Figure 1a; the connection between homologous motor areas in this example) is interrogated using diffusion-weighted imaging (Figure 1b). Due to the sizes of the underlying axons within the white matter relative to the imaging resolution, there will typically be of the order of a million axons traversing any given image voxel.

The notion of a single scalar quantity of 'connectivity' of a white matter pathway is intrinsically ambiguous. If quantifying such a property of the underlying biological bundle, a reasonable interpretation would be the *number of axons* constituting the connection, as the information-carrying capacity of the bundle could be reasonably expected to scale in direct proportion to such. However, precisely estimating this parameter is prohibited by the limitations of diffusion-weighted imaging (DWI). The logic behind the proposed *total intra-axonal cross-sectional area* metric mentioned here in Figure 1 is discussed further in the 'Metric of "connectivity"' section.

- A diffusion model estimates from these data, within each image voxel, the orientations and densities of the fibre bundles within that voxel (Figure 1c–d).
- These orientation estimates are used by a streamlines tractography algorithm to attempt to reconstruct in

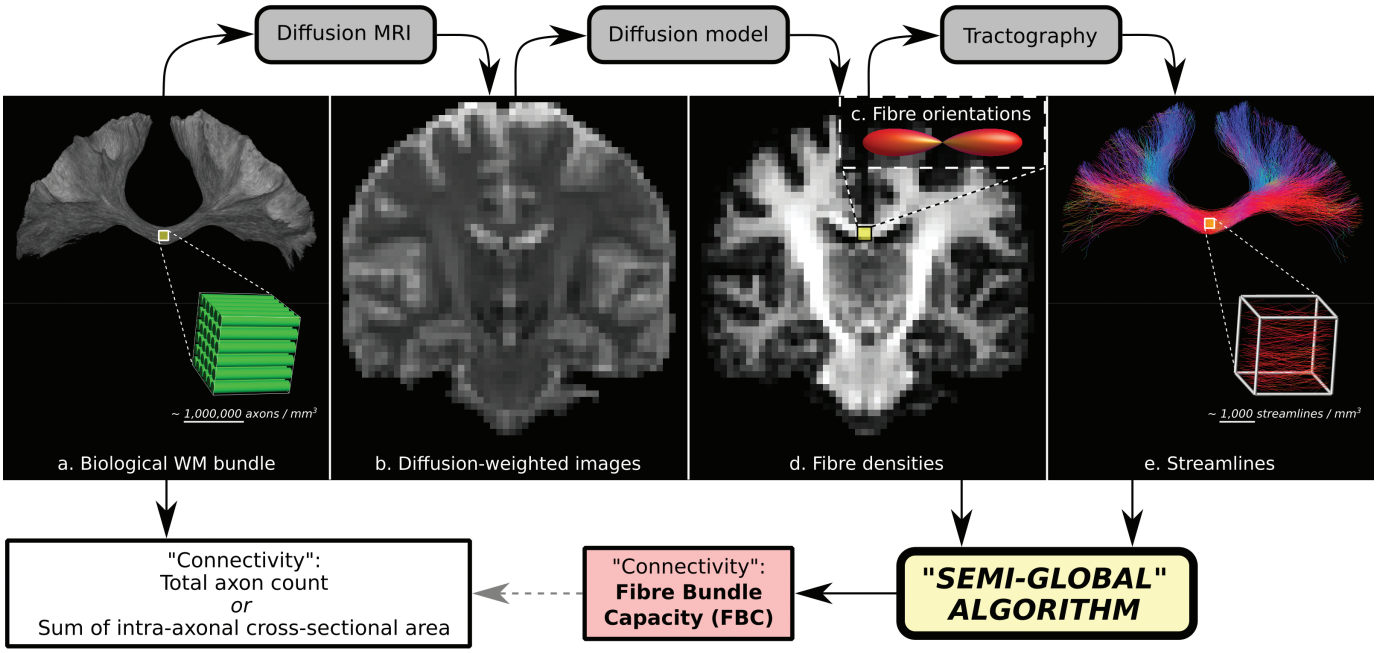

Fig. 1. Contextualisation of semi-global tractogram optimisation algorithms. Given the existence of a biological white matter pathway of interest (a), diffusion-weighted imaging is performed (b). A diffusion model is fitted to these data to yield fibre orientation (c) and density (d) estimates. Fibre orientations are utilised by a tractography algorithm to produce streamlines (e). An optimisation algorithm operates on both the tractogram reconstruction and FD information to yield an estimate of bundle connectivity, here named 'fibre bundle capacity (FBC)', which should ideally be proportional to the connectivity of the biological bundle.

a piecewise fashion the fibres within the pathway of interest (Figure 1e). Unlike biological axons, reconstructed streamlines have no associated volume and are therefore shown as infinitesimally thin in Figure 1e. The number of streamlines traversing any given image voxel may be of the order of 1,000, but varies wildly depending on reconstruction parameters.

- The role of such a 'semi-global' tractogram optimisation algorithm is to combine the reconstructed tractogram with fibre density (FD) information from the diffusion model (or alternatively the diffusion-weighted image data themselves; see the 'Comparing tractograms and image data' section), relying on the quantitative nature of these FD estimates to overcome the non-quantitative nature of streamlines tractography.
- The outcome of such a process is a derived measure of 'connectivity' of the pathway of interest (here named 'fibre bundle capacity (FBC)'; more in the 'Metric of "connectivity"' section). If calculated appropriately, this measure should be a reasonable proxy for the information-carrying capacity of the biological pathway.

Unlike other analysis techniques that interrogate the values of quantitative properties *as they vary along the length* of a white matter bundle of interest,[34–39] here the derived experimental output is a *single scalar measure* reflecting the *total* 'connectivity' of that pathway between its two endpoints.

While this explanation (and subsequent demonstrations in this article) focuses on performing such a quantification for only a single pathway of interest, all of the content of this article is directly relevant to the construction and subsequent interrogation of the brain 'structural connectome'.[23,24] Within this framework, a parcellation of the grey matter is defined, and for every possible unique pair of grey matter regions, a scalar measure of 'connectivity' is quantified, with these values together forming a *connectivity matrix* that encodes the value of this connectivity metric between pairs of regions in their corresponding rows/columns.[29,30,40] Such connectome construction can therefore be thought of as simply *repeating this quantification process many times*, where each 'bundle of interest' is defined based on the streamline endpoints being ascribed to a specific pair of grey matter regions. So, in the context of connectomics, the techniques described here for characterising such 'connectivity' are intended to:

- Supersede the use of streamline count, which continues to be used in neuroscientific applications despite being known to be biased by many reconstruction-related parameters[10,19,41];
- Provide a measure of 'connectivity' for which, when applying higher-order analyses that implicitly interpret such data as the bandwidth of information flow around a network,[42,43] such an interpretation is more direct and intuitive than alternative measures such as aggregate microstructural quantities.

Metric of 'connectivity'

The notion of 'connectivity' in the context of diffusion MRI tractography remains ambiguous without a very explicit description of exactly what metric is derived from

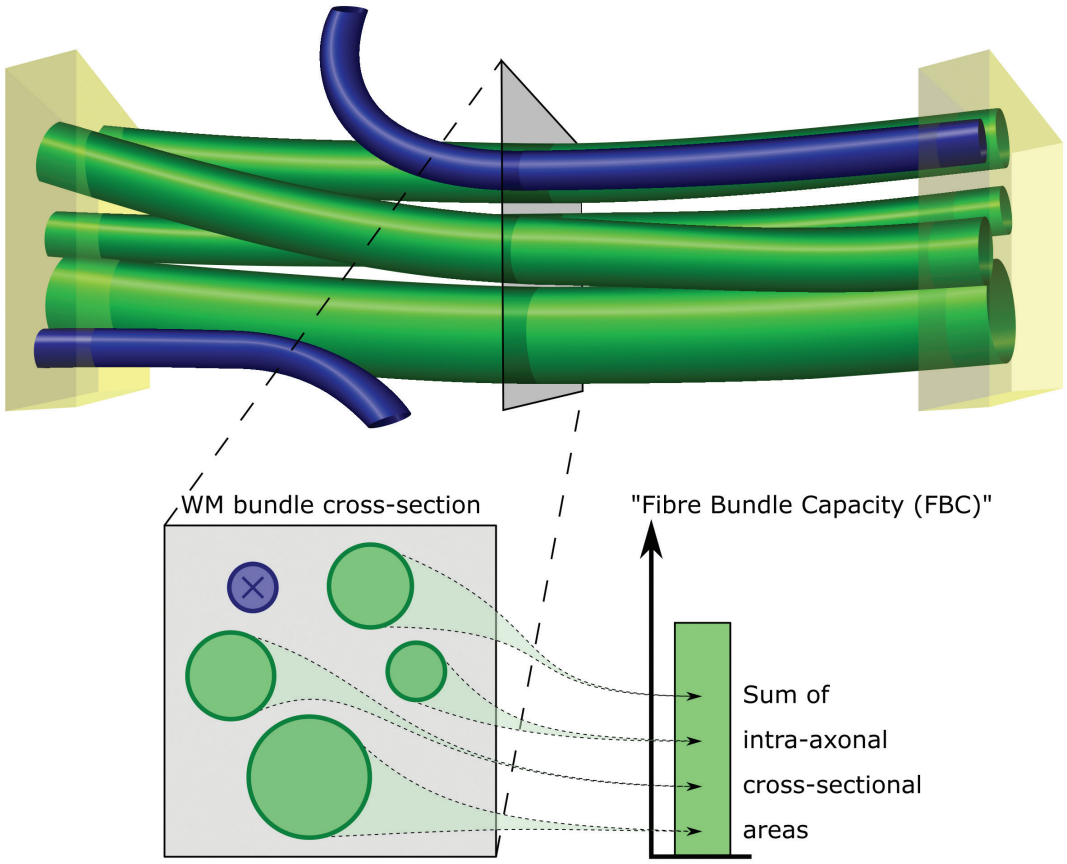

Fig. 2. Visual depiction of the fibre bundle capacity (FBC) metric. A white matter bundle of interest is defined based on its endpoints, shown as yellow cuboids. Only those fibres that are attributed to *both* endpoints are constituent members of that bundle (green cylinders). The FBC is defined as the sum of the intra-axonal cross-sectional areas of these fibres.

the image data/tractogram reconstruction. In the diffusion MRI tractography literature, myriad metrics have been utilised, all of which have been referred to at some point as simply 'connectivity'.

In the context of the methods discussed here, our target scalar metric of interest when quantifying 'white matter connectivity' is the *total fibre cross-sectional area* of a fibre bundle (ideally, the *intra-axonal* cross-sectional area). The nature of this metric is presented visually in Figure 2, where a bundle of interest is defined based on those fibres connecting two endpoints of interest, and the intra-axonal cross-sectional areas of *only those fibres attributed to the bundle of interest* are summed to derive this estimate. This metric has previously been shown to converge white matter connection density estimates towards gross axon count estimates from *post mortem* dissection.[44] To facilitate discussion of higher-level concepts in the context of this metric, we henceforth refer to this metric as the 'FBC'. This term communicates that the intent of this measure is the capacity of a white matter fibre bundle to transmit information between its endpoints. Ideally, derivation of this measure should be as sensitive and specific as possible to the intra-axonal cross-sectional area of the biological fibres constituting the pathway being reconstructed. While for simplicity this metric can be thought of as a proportional estimate of axon *count*, the precise attributes of this metric are discussed later in the 'Qualifying the "Fibre Bundle Capacity (FBC)" metric' section.

The important distinction between FD estimates quantified at the *voxel* level, and fibre *connection* density estimates (i.e. FBC) quantified at the level of *pathways of interest*, is demonstrated in Figure 3. There are various diffusion models that include some parameters related to fibre volume for each image voxel (Figure 3a–d). In the context of this article, however, we seek to quantify the total fibre cross-sectional area associated with some specific pathway of interest (Figure 3e–f).

Limitations of semi-global optimisation algorithms

- We do not consider the sub-voxel spatial configurations of fibre bundles in either the image[45] or tractogram[46] domains; we consider only that each voxel is the sum of its constituent parts, irrespective of sub-voxel position;

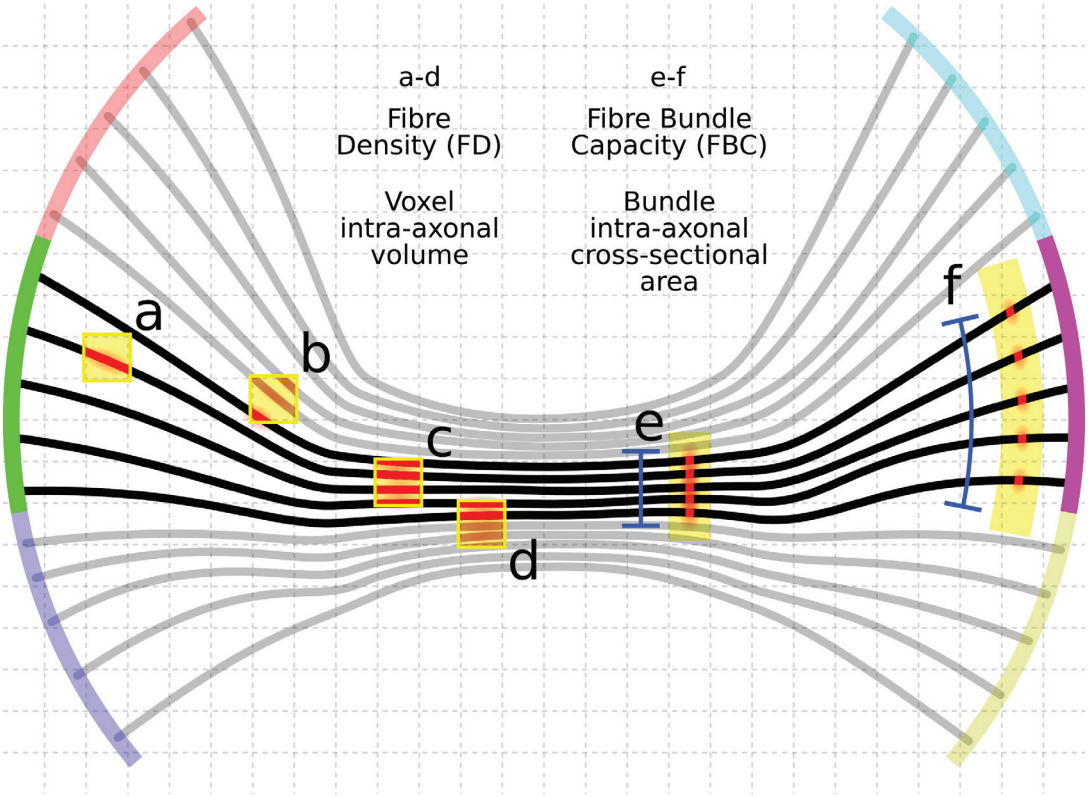

Fig. 3. Relationship between quantification of intra-axonal volume within individual voxels (FD), and quantification of intra-axonal cross-sectional area of a white matter bundle of interest (fibre bundle capacity (FBC)). A bundle of interest is defined based on selection of two parcels (yellow surfaces) within a grey matter surface segmentation (planes at far left and far right of the figure). (a) A diffusion model may provide, within each individual image voxel, an estimate of intra-axonal volume (FD). Any bundle of interest will likely traverse a large number of image voxels along its length and breadth. (b) The parameter of interest for quantifying the 'connectivity' of this white matter pathway is the total intra-axonal cross-sectional area of the axons attributed to the bundle of interest (FBC). Note that this is irrespective of the length of the pathway or the total dimensions of the plane necessary to encapsulate all axons within that pathway.

- We assume that the diffusion signal measured in a voxel is the sum of signal contributions from the matter fibre bundles and other tissues within that volume (i.e. the 'slow exchange' regime);
- We do not consider influencing streamlines *trajectories* based on microstructural information, as discussed[47] and proposed[48] recently; we consider only the use of microstructural/image information to *modulate the reconstructed densities of different white matter pathways*.

Comparing tractograms and image data

Throughout this discussion, we use the term '*fixel*'[49] to refer to a specific *f*ibre population within a particular vox*el*. Each voxel in the diffusion image may contain multiple fixels ('crossing fibres'), and the number of fixels may vary between different voxels. Use of such terminology assists in disambiguating this concept from a macroscopic white matter *fascicle* that connects two areas of grey matter, each of which will be associated with many fixels along its length and breadth.

Using diffusion image data to provide a tractogram with quantitative attributes requires a mechanism by which to compare the tractogram to those image data. There are two principal mechanisms by which this may be done (demonstrated in Figure 4):

1. Each streamline contributes some intensity to the reconstructed diffusion signal based on a *forward model*. Typically, a diffusion tensor with fixed diffusivities is chosen. Signal intensity from sources other than white matter fibres may additionally be modelled as isotropic or anisotropic sources contributing to the diffusion signal and included in the optimisation. The reconstructed image data from the tractogram (and possibly other tissue sources) is compared directly to the empirical diffusion data.
2. The white matter fibre density within each fixel is first estimated based on an *inverse model*, potentially with estimation and separation of other signal sources (e.g. other tissues or fluid).[50–58] Here, we focus on the spherical deconvolution model,[31,59,60] though other approaches can certainly be used. The reconstructed streamlines density from the tractogram ascribed to each fixel is compared directly to the corresponding white matter fibre densities estimated from the diffusion model.

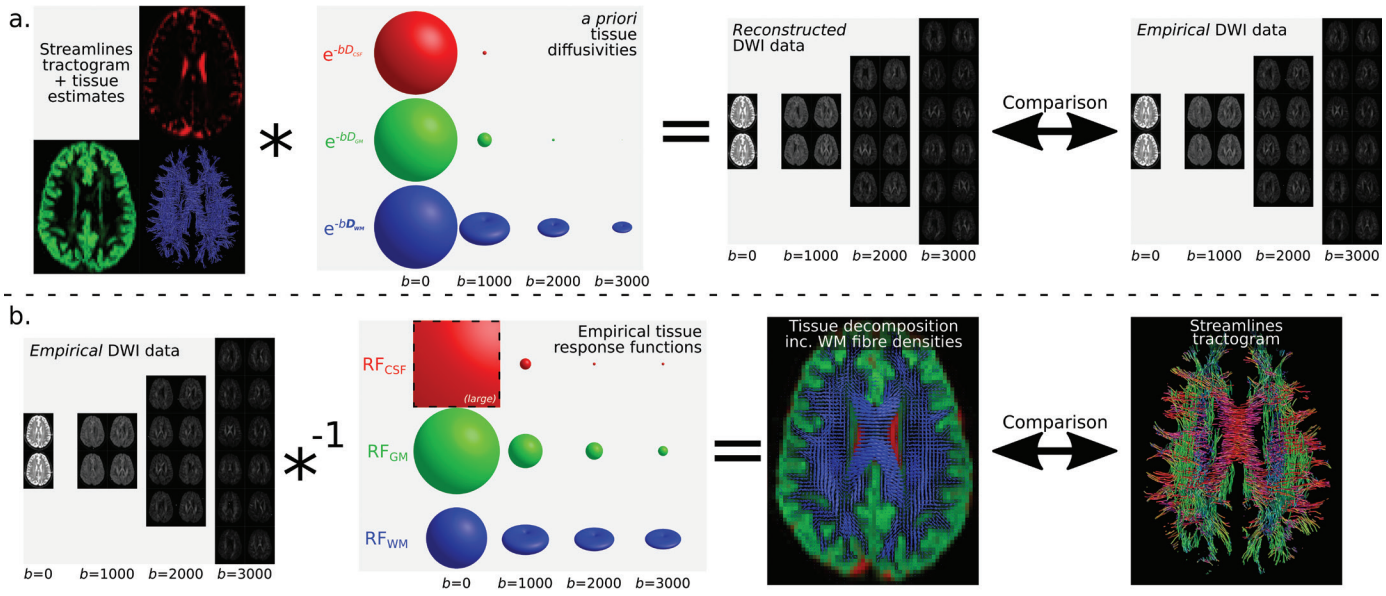

Fig. 4. Relationship between two different modelling approaches used in 'semi-global' tractography optimisation algorithms. (a) Based on estimates of local densities of different types of tissue (including orientation information in the case of white matter streamlines), and functions describing how each tissue contributes to the diffusion signal at different *b*-values (often derived from e.g. the diffusion tensor model), a spherical convolution is performed to estimate the diffusion signal from the current tractogram reconstruction. This is compared to the empirical diffusion signal intensity data, and the tissue density estimates within the reconstruction are revised accordingly. (b) Based on tissue response functions describing the appearance of each type of tissue in the diffusion data (determined either from some model or from the image data directly), a spherical deconvolution is performed to obtain estimates of tissue densities (including orientation information in the case of white matter fibres). The densities of a reconstructed tractogram are compared to the white matter fibre density estimates, and the parameters of the tractogram are revised accordingly.

Although the former approach is more 'conventional', and additionally has a long history of use in the context of global tractography methods, for demonstration purposes we use the latter model, as it provides a more intuitive course of reasoning in the following sections.

Note that these two approaches are directly related via the invertibility of the spherical convolution transform: the *a priori* definition of the forward models to be used for each tissue component/compartment in approach (1) serves the same purpose as the *a priori* definition of the tissue 'response functions' for spherical deconvolution in approach (2) (Figure 4). Note also that in Figure 1, the 'semi-global algorithm' is shown to be utilising information from estimated fibre densities rather than the diffusion-weighted images, corresponding to case (2) described here.

There is an important difference between these two cases that is requisite for proper understanding of subsequent sections of this article. In mechanism (1), the model considers not only the *density* of streamlines within any particular image voxel, but also the *precise orientation distribution* of those streamlines: the contribution of each streamline towards the reconstructed diffusion-weighted signal is based on the tangent of the streamline at each location along its trajectory. In mechanism (2), the diffusion model defines a small finite number of discrete fixels in each image voxel; the algorithm that maps each streamline to the DWI voxel grid[19] determines the orientation of each streamline-voxel intersection, which is then attributed to the appropriate fixel within that voxel. As such, each streamline has associated with it a set of fixels traversed, and each fixel has associated with it both an FD as estimated by the diffusion model and a total streamlines density based on the set of streamlines traversing it. The algorithms described below involve direct utilisation of this per-fixel information (to a greater or lesser extent). While mechanism (1) is potentially sensitive to fibre/streamlines orientation distribution information that is more complex than what can be represented using a small finite number of discrete fixels in each voxel, mechanism (2) essentially utilises the fixels provided by the diffusion model as a sparsifying transform, reducing the size of the computational problem; further, the fact that it is possible to perform for each fixel a direct scalar comparison between FD and total streamlines density makes this mechanism more amenable to promoting an understanding of the logic underlying the methods described in this article.

METHODS

The algorithmic basis of quantitative streamlines tractography

In order to demonstrate the fundamental operation of the algorithms under discussion (and hence the quantitative properties they provide), we begin with a simple

definition of the fundamental data and research question that may be applicable to an example analysis involving diffusion MRI tractography.

- What we *want*:
  - An estimate of the FBC metric for some pathway, as defined in the Background section and demonstrated in Figures 2 and 3.
- What we *have*:
  - A measure of fibre volume for each fixel as estimated via a diffusion model;
  - A set of streamlines delineating the trajectory of the pathway of interest, typically based on *a priori* regions of interest or other criteria to isolate the pathway;
  - A whole-brain tractogram, of which the set of streamlines ascribed to the pathway of interest is a subset (while this is not required for Algorithm 1, its necessity will be demonstrated in later algorithms).

The example to be used for demonstration in this article is the connection between left and right precentral sulci, as derived from the 'Desikan-Killiany' parcellation[61] provided by the FreeSurfer software[62]; this is shown in Figure 5.

We now demonstrate in this section several plausible algorithmic approaches by which our goal may be achieved. We start by proposing a relatively simple and naïve algorithm, observing its benefits and shortcomings, and then use these observations to derive increasingly advanced approaches, eventually presenting a total of four algorithms.

Algorithm 1: 'Fixel mask'

Algorithm 1 is the simplest possible approach for incorporating the FD information from a diffusion model into estimating FBC for a pathway of interest reconstructed using streamlines tractography. It is based on the observation that a pathway *volume* can be derived by computing a *mask* of fixels that are traversed by the streamlines belonging to that pathway, and this can be converted to a pathway *cross-sectional area* based on the *length* of the pathway (Figure 6; see also pseudocode in Appendix):

Step 1. Identify all fixels that are traversed by at least one streamline belonging to the pathway.
Step 2. Sum the fibre volumes of all selected fixels to calculate the total fibre volume of the pathway.
Step 3. Divide this value by the mean streamline length to estimate FBC for the pathway.

Figure 7a shows the assignment of FD from the underlying diffusion model field to the quantification of volume (and hence cross-sectional area) of this specific pathway. There are a couple of weaknesses in this algorithm observed in Figures 6 and 7a:

- The effect of 'outlier streamlines': those streamlines that are attributed to the pathway of interest but follow a trajectory drastically different from the rest of the streamlines assigned to the pathway. When this occurs, *all* of the fixels traversed by that streamline are added to the fixel mask, and *all* of the FD within each of those fixels contributes to the total fibre volume of the pathway. One or a small number of stray streamlines may therefore drastically increase the final quantification of FBC (e.g. the streamline in Figure 5 that travels partway down the corticospinal tracts as it traverses between the two regions of interest).

  Utilisation of some more stringent criteria for inclusion of fixels in the mask (e.g. an increased streamline count threshold) could theoretically mitigate this effect, though what form such criteria should take is subjective. Alternatively, such errors may be addressed using additional tractography regions-of-interest or manual quality control procedures; but such mitigation does

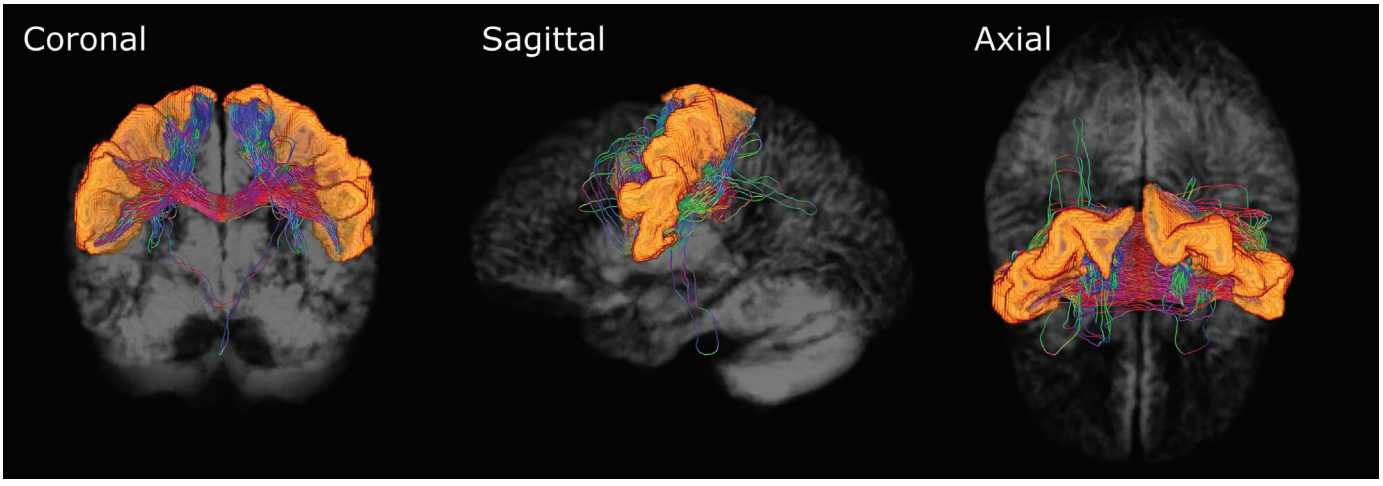

Fig. 5. Visualisation of the pathway of interest to be used in a demonstration of the four fibre bundle capacity (FBC) quantification algorithms presented in the 'Methods' section: three orthogonal views. The left and right precentral sulci are highlighted in orange; streamlines are coloured according to their local tangent orientation (red = left-right; green = anterior-posterior; blue = inferior-superior).

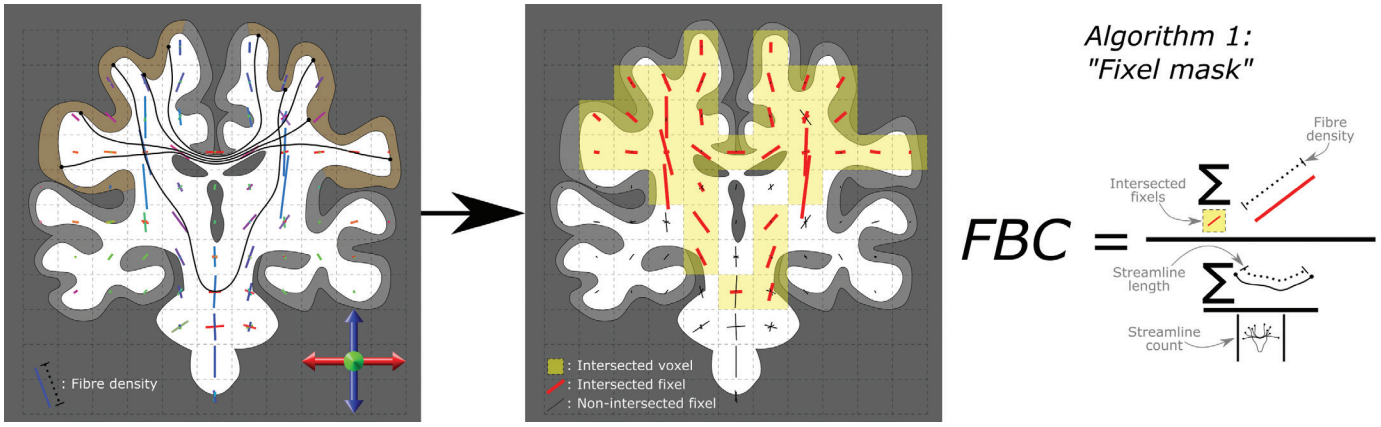

Fig. 6. Visual demonstration of the operation of Algorithm 1 ('Fixel mask'). For a particular pathway of interest (left panel: grey matter regions labelled orange, leading to selection of streamlines shown), those fixels traversed by the streamlines corresponding to that pathway are selected (right panel: red fixels within yellow voxels). The sum of the microscopic fibre densities of these selected fixels (equation numerator; encoded visually as fixel lengths) is divided by the mean streamline length (equation denominator: sum of streamline lengths divided by the number of streamlines) to yield the fibre bundle capacity (FBC) measure.

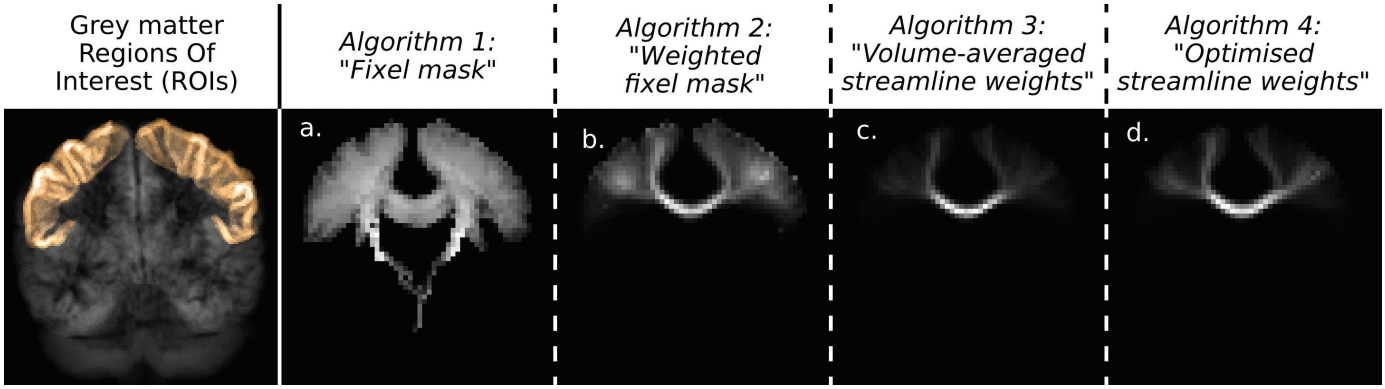

Fig. 7. (Left) Coronal projection of brain grey matter, with regions of interest used in the reconstruction of the pathway of interest highlighted; (a–d) Maximum intensity projection (MIP) spatial distributions of the density of white matter fibres attributed to the pathway of interest resulting from quantification using the four algorithms described in the 'Methods' section. The reconstructed bundle is that shown in Figure 5.

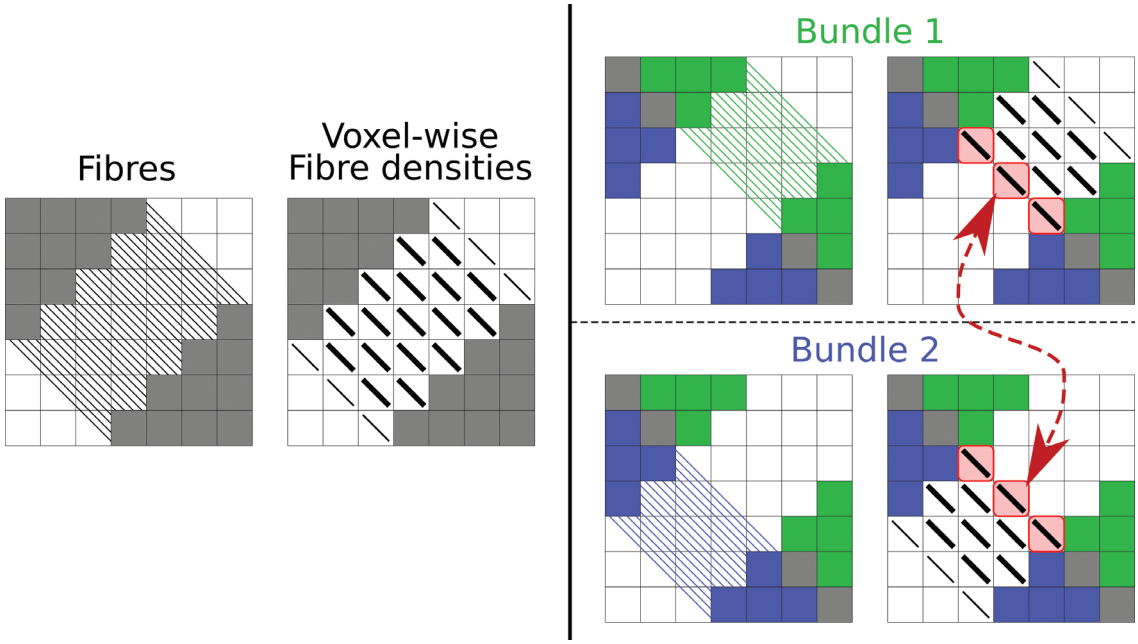

Fig. 8. The effects of partial volume on Algorithm 1. Left: A white matter fibre pathway connecting between two grey matter regions, shown as both fibre trajectories and per-voxel fibre orientation/density. Right: The pathway is split into two bundles of interest based on parcellation of the voxels at the endpoints of the pathway; a subset of voxels (highlighted red) is intersected by both bundles.

not trivially extend to studies where many different pathways are assessed (e.g. when building the structural connectome over the whole brain).

- The local FD per voxel attributed to the pathway is relatively consistent throughout the entire pathway, from the corpus callosum through the centrum semiovale and to the interface between grey and white matter. This is, however, contrary to how such tracts are constructed physically: as white matter fibres fan out from the narrow cross-section of the corpus callosum to a long strip of grey matter, the local voxel-wise density of the fibres within this specific pathway would be expected to decrease.

The way in which these effects can manifest, as well as the source of the limitation, is demonstrated in Figure 8. Here the selection of two bundles of interest from a larger white matter pathway is shown, both in the corresponding streamlines and in the fixels to which they are ascribed. What is highlighted in red is the fact that if each of the two bundles is independently mapped to the corresponding voxels traversed, then for the set of voxels intersected by both bundles, *all* of the FD within those voxels will be attributed to *both* bundles. This has two effects: firstly, the spatial distribution of FD attributed to each bundle individually does not vary smoothly, failing to represent partial volume at the outer edge of each bundle similarly to that observed in Figure 7a; secondly, the sum of the calculated fibre connectivity of the two bundles would be greater than that of the actual white matter structure — without even necessitating tractography reconstruction errors — as the FD in those voxels would contribute to the quantification of both bundles.

Algorithm 2: 'Weighted fixel mask'

Algorithm 2 directly addresses the major imperfections of Algorithm 1 that arise due to partial volume effects. It is based on the observation that when a fixel is traversed by streamlines belonging to the pathway of interest *in addition to* other streamlines *not* belonging to that pathway, then rather than the *entire fibre volume* of that fixel contributing to the pathway, ideally only the *fraction of that fixel attributed to the pathway of interest* should be included. This is achieved as follows (Figure 9; see also pseudocode in Appendix):

Step 1. Generate a whole-brain tractogram; define the pathway of interest as a *subset* of those whole-brain streamlines.
Step 2. For every fixel, calculate the *fraction of the total streamlines density* in that fixel that belongs to the pathway of interest.
Step 3. The contribution of the fibre volume of each fixel to the fibre volume of the pathway of interest is modulated by the fraction of that fixel ascribed to the pathway of interest in step 2.
Step 4. As in Algorithm 1, divide the total volume of the pathway by the mean streamline length to estimate FBC.

The primary advantage of this approach over Algorithm 1 is that if a fixel is only traversed by a small number of streamlines within the pathway of interest, that fixel only contributes a small amount of its fibre volume to the FBC result. The effect of this change from Algorithm 1 is particularly evident in the inferior half of the brain in Figure 7b, where individual erroneous streamlines trajectories contribute far less to the calculated fibre pathway volume.

While various streamline reconstruction biases mean that the fixel fibre volume fractions ascribed to the streamlines within the pathway of interest may not be precisely equivalent to the total fraction of the *underlying fibres* within that fixel that belong to the *biological* pathway of interest, this algorithm certainly provides a

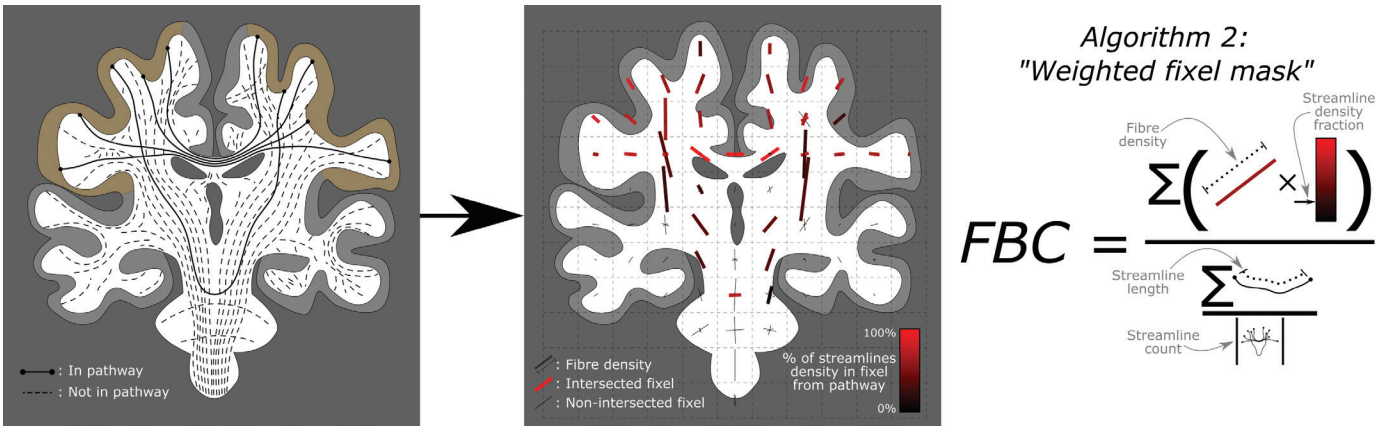

Fig. 9. Visual demonstration of the operation of Algorithm 2 ('Weighted fixel mask'). The streamlines corresponding to the pathway of interest (left panel: solid lines) are a subset of a whole-brain tractogram (left panel: dashed lines). For each fixel in the image (right panel), the fraction of the streamlines density in that fixel corresponding to the pathway of interest can be quantified (right panel: red intensity). The contribution of the fibre volume within each fixel (encoded visually as fixel lengths) to the pathway of interest is modulated by the fraction of the streamlines density in that fixel attributed to the pathway of interest (multiplication in equation numerator); as with Algorithm 1, this volume is then divided by the mean streamline length (equation denominator: sum of streamline lengths divided by the number of streamlines) in the calculation of fibre bundle capacity (FBC).

perceptible improvement over Algorithm 1, with the spatial distribution of fibre volume within the pathway having a much more biologically plausible appearance.

An inherent problematic issue in the design of Algorithm 2, however, is that it *fails to enforce a consistent intra-axonal cross-sectional area* within the pathway. Along the length of the fibre bundle shown in Figure 7b, there are local 'hot-spots' of supposedly increased fibre volume, both within the superficial white matter and where the bundle intersects the grey matter targets. While individual axons may have some modulation in their diameter along their length, such gross modulation of macroscopic intra-axonal cross-sectional area is *physically unrealistic* for white matter pathways at the macro-scale. Observation of such in diffusion MRI data is therefore far more likely to be an artefact of image analysis and reconstruction. Furthermore, at the endpoints of the pathway, voxels containing partial volume between grey and white matter are likely to contain a smaller number of streamlines than those voxels entirely within the white matter, which results in the fraction of fixel FD assigned to the pathway of interest being prone to quantisation effects; this contributes to the 'speckly' appearance of the density map in Figure 7b near the grey matter.

Algorithm 3: 'Volume-averaged streamline weights'

In order to overcome the fundamental limitation of Algorithm 2, a solution is sought for deriving FBC that *enforces a constant intra-axonal cross-sectional area* along the length of the pathway. We clarify here that this constraint does *not* apply to the macroscopic span of space traversed by fibres of that bundle, but applies specifically to the *intra-axonal* portion of the bundle. For example: when fibres within a tightly packed bundle diverge from one another (commonly referred to as 'fanning'), the surface area of the subset of a plane encapsulating all fibres in the bundle may increase (the 'macroscopic cross-section'), but the sum of intra-axonal cross-sectional areas should remain *unchanged* if the axon diameters are consistent along their length (e.g. Figure 2; Figure 3e–f); here it is the *latter* definition that we advocate should be constrained.

Algorithm 3 is an initial realisation of this concept. It enforces constant intra-axonal cross-sectional area of the pathway, by requiring that each *streamline* in the pathway contributes a *constant fibre cross-sectional area* along its entire length. Hence, unlike Algorithms 1 and 2, here contributions towards FBC are made not per *fixel*, but per *streamline* (in the context of semi-global tractography algorithms, these parameters are sometimes referred to as 'weights').

This algorithm operates as follows (Figure 10; see also pseudocode in Appendix):

Step 1. Using the whole-brain tractogram, calculate the total streamlines density in each fixel.

Step 2. For each streamline, calculate the *fibre volume* to be attributed to that streamline. Every fixel traversed by the streamline contributes a fraction of its fibre volume to the sum for that streamline, based on the fraction of the total streamlines density in that fixel that was contributed by that particular streamline.

Step 3. Convert the *fibre volume* of each streamline to a *fibre cross-sectional area*, by dividing by the length of that streamline.

Step 4. Sum the cross-sectional areas of the streamlines belonging to the pathway of interest to derive FBC.

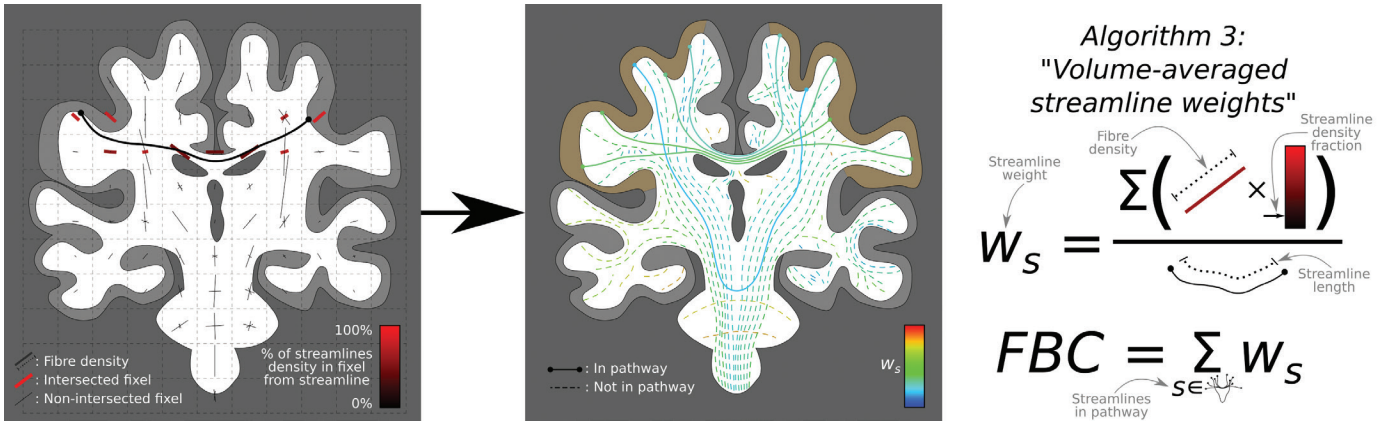

Fig. 10. Visual demonstration of the operation of Algorithm 3 ('Volume-averaged streamline weights). For each individual streamline, the total fibre volume attributed to that streamline (numerator, first equation) is based on the products of the fixel fibre volumes (encoded visually as fixel lengths) and the fraction of the streamlines density in each of those fixels attributed to the streamline of interest (left panel: encoded as red intensity); this fibre volume is then divided by the length of that individual streamline (denominator, first equation) to ascribe a 'weight' w_s to each individual streamline s (right panel: streamline colours). The fibre bundle capacity (FBC) of the pathway of interest is then the sum of the weights ascribed to the streamlines attributed to the pathway of interest (right panel: solid lines).

While this algorithm produces a measure of fibre cross-sectional area per streamline rather than fibre volume per fixel, it is still possible to reconstruct the latter; this allows us to generate a spatial map of FD attributed to the pathway of interest that can be compared to Algorithms 1 and 2. The *product* of a cross-sectional area with a length yields a measure of *volume*; hence, each streamline in the tractogram contributes a fibre volume to every voxel it traverses, based on the product of its weight and the length of the streamline segment that intersects that voxel. The result of this process is shown in Figure 7c. Compared to the previous two algorithms, this approach produces an FD map for the resulting pathway that appears quite biologically reasonable, with a maximal microscopic FD within the narrow confines of the corpus callosum that decreases as those fibres fan out towards the cortex.

There does, however, remain one slight inadequacy with this algorithm. Consider an experiment where, instead of deriving a spatial map of reconstructed fibre volume for a particular pathway of interest only (as we have been doing here), we instead map the spatial distribution of reconstructed fibre volume *of the entire tractogram*. If the streamlines weights are faithful to the intra-axonal cross-sectional areas of the biological fibres following the trajectories reconstructed by those streamlines, then one would expect an *accurate reproduction* of the fibre volumes that were estimated from the voxel-wise diffusion model throughout the white matter (or equivalently: applying the forward model to the whole-brain tractogram should yield the empirical diffusion signal, as demonstrated in the 'Comparing tractograms and image data' section and Figure 3). Note this process is very similar to track density imaging (TDI) at native DWI resolution,[63–65] incorporating the ability for streamlines to contribute differentially towards the image.

This experiment is shown in Figure 11. The reconstructed FD from the outcome of Algorithm 3 (Figure 11c) is closer to the voxel-wise estimate of white matter FD derived from spherical deconvolution (Figure 11a) than the original tractogram where every streamline contributes equally (Figure 11b). However, it still does not provide an entirely faithful representation of the underlying white matter FD field. This is perhaps expected given the nature of the algorithm itself. From a physical perspective, the operation of this algorithm can be thought of as taking the sum of fibre volumes attributed to the streamline by each fixel (which may be greater or lesser at different points along the streamline) and *spreading* this fibre volume evenly along the length of the streamline in order to ascribe to it a *constant* fibre cross-sectional area. While this process does go *some way* to incorporating fibre volume information from the diffusion model into the tractogram, it *fails to directly enforce consistency* between the estimated FD and reconstructed streamlines density for each fixel of the image (the residual discrepancy visible between Figure 11a and 11c). In the case of the specific pathway of interest used in this demonstration, the FD within the corpus callosum projected by the tractogram is clearly greater than that indicated by the image data; this means that the calculated FBC for this connection relative to other pathways when using Algorithm 3 would likely be an over-estimate.

Algorithm 4: 'Optimised streamline weights'

Addressing the remaining problem with the approach described in Algorithm 3 — the fact that the fibre volumes estimated from the tractogram are not a sufficiently accurate reconstruction of the fibre volumes estimated from the diffusion model, as shown in Figure 11 — is a fundamental requirement if we are to consider the streamline weights truly quantitative. If the streamlines trajectories and ascribed weights are reflective of the underlying biological connectivity, then the spatial distribution of FD throughout the white matter represented within this connectivity-based reconstruction should accurately match estimates of this measure that are derived from the image data directly.

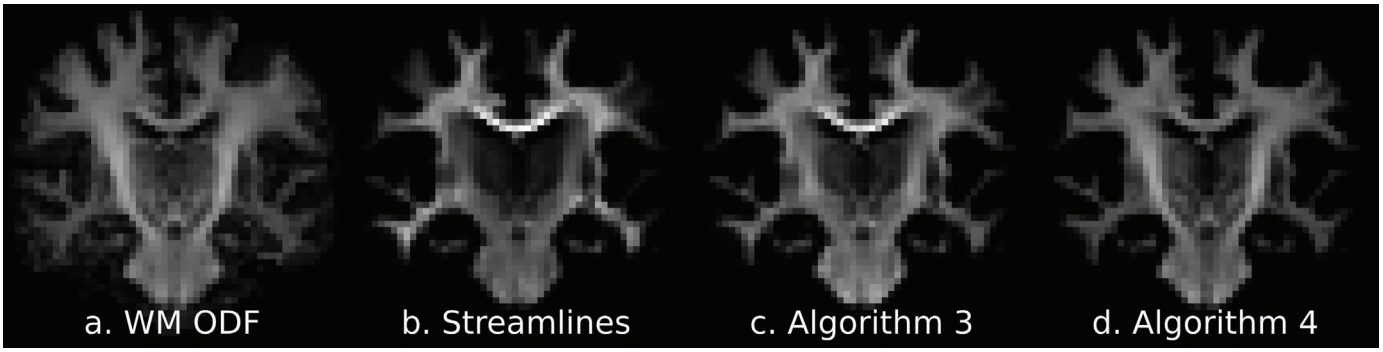

Fig. 11. Comparison of spatial distributions of track densities from whole-brain tractogram data with the density of white matter fibres as estimated through spherical deconvolution. (a) The orientationally averaged mean of the white matter orientation distribution functions (the l=0 term of the spherical harmonic expansion) as a measure of total fibre density within each voxel. The distribution of TD within a whole-brain tractogram should ideally match these data. (b–d) The density of streamlines in the whole-brain tractogram when the contribution of each streamline to the map is modulated as follows: (b) no modulation (all streamlines contribute equally); (c) modulated by the weights ascribed to the streamlines by Algorithm 3 ('Volume-averaged streamline weights'); (d) modulated by the weights ascribed to the streamlines by Algorithm 4 ('Optimised streamline weights').

This limitation is addressed by designing an algorithm that *explicitly* seeks to derive a set of streamline weights that result in an accurate reconstruction of the underlying fibre volumes estimated from the diffusion model (or equivalently, an accurate reconstruction of the empirical diffusion signal using a forward model). This basic concept is shown diagrammatically in Figure 12 and might proceed, for example, as follows (see also pseudocode in Appendix):

Step 1. Initially assign a unity weight to each streamline.
Step 2. Using the whole-brain tractogram, based on the current streamline weights, calculate the total streamlines density in each fixel.
Step 3. For each fixel, calculate the difference between the FD estimated from the diffusion model and the total attributed streamlines density.
Step 4. For each streamline, increase or decrease the weight in order to minimise the error quantified in step 3.
Step 5. Loop back to Step 2 until some termination criterion is met.
Step 6. Sum the weights of those streamlines belonging to the pathway of interest to derive FBC.

This is the mechanism by which the 'spherical-deconvolution informed filtering of tractograms 2 (SIFT2)' method[22] operates. The spatial distribution of FD within the pathway of interest after having applied the SIFT2 algorithm is shown in Figure 7d, and the spatial distribution of FD of the entire tractogram is shown in Figure 11d. Crucially, the latter demonstrates a highly accurate reproduction of the underlying FD field estimated from the diffusion model (Figure 11a), highlighting how this approach provides a tractogram-based connectivity model that obeys the fundamental spatial constraints imposed by the physical nature of the underlying biological fibre structure. It is this observation that permits the streamline weights estimated by such algorithms to be used in the quantification of FBC (within the constraints imposed by other limitations associated with diffusion MRI streamlines tractography[66]).

Inter-subject connection density normalisation

Whenever quantitative data are to be compared across subjects, an important distinction must be made between *absolute* and *relative* quantitative measures. For instance, when assessing the fractional anisotropy (FA) measure[67] from the diffusion tensor model,[68] there is no need to modulate these values differentially between subjects, as it is an *absolute* measure (for any given DWI acquisition scheme) and therefore any differences in this metric between individuals can be interpreted according to the properties encapsulated within that metric. However, if a quantitative measure is *relative* to other latent parameters that vary across individuals, care must be taken to appropriately handle the effects of those latent parameters, in order to be able to interpret any

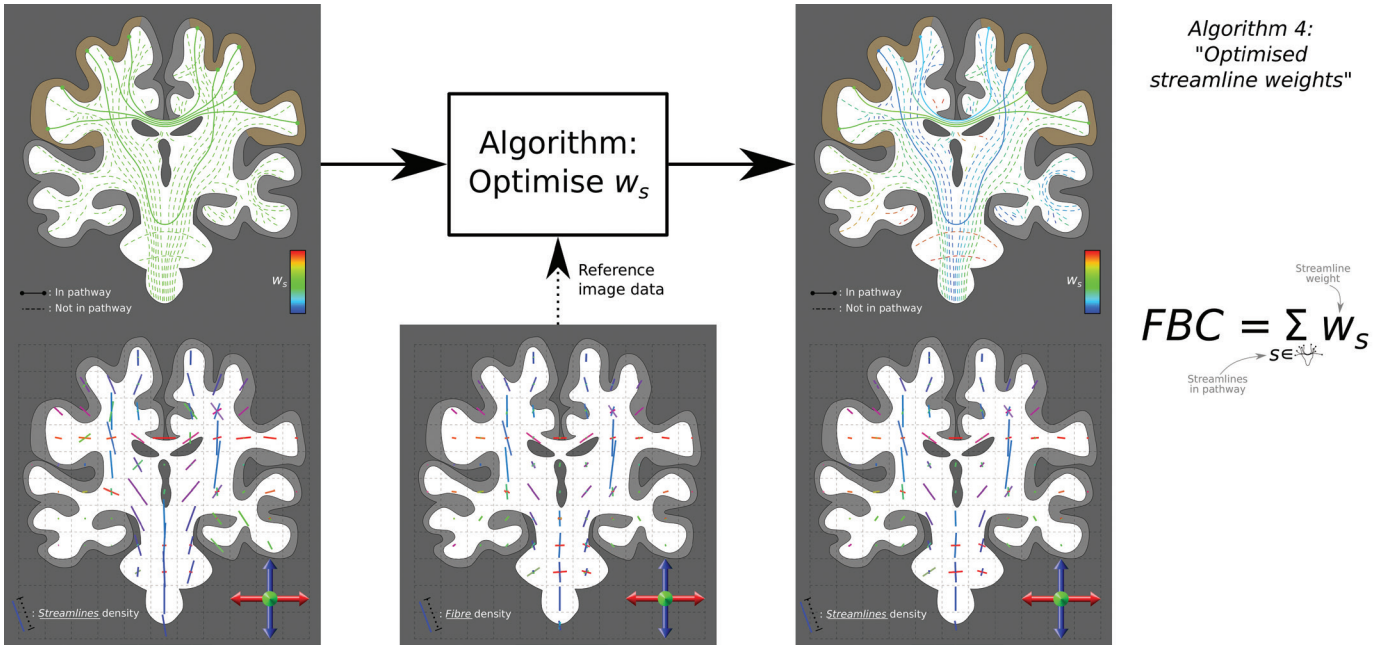

Fig. 12. Visual demonstration of the operation of Algorithm 4 ('Optimised streamline weights'). For a whole-brain tractogram (top left panel), the total streamlines density traversing each fixel (bottom left panel; encoded visually as fixel lengths) may not match the fibre volumes estimated from the diffusion model (bottom panel; fixel lengths). This algorithm modulates the weight w_s ascribed to each streamline s (top right panel: streamline colours) in order to achieve correspondence between the total streamlines density traversing each fixel (bottom right; fixel lengths) and the diffusion model fibre density estimate (bottom panel). The fibre bundle capacity (FBC) measure for the pathway of interest is the sum of the weights ascribed to those streamlines attributed to the pathway of interest (top right panel; solid lines only; streamline colours).

differences in that metric as being *specific* to that metric rather than some nuisance confound.

In the fixel-based analysis (FBA) framework,[69] which enables statistical analysis of white matter quantitative measures in the presence of crossing fibres, FD estimates must be comparable across subjects throughout some common template space. In the context of apparent fibre density (AFD) quantification[70] using the spherical deconvolution model,[59] the fibre orientation distributions (FODs) (i.e. the representation of estimated fibre directions and densities in each voxel) are deliberately *not* normalised either to a unit integral in each voxel or to the intensity of the *b*=0 image (i.e. volume acquired with no diffusion sensitisation) in each voxel. This makes the size of the FOD directly proportional to the magnitude of the DWI signal (which is itself proportional to intra-cellular volume at high *b*-values[70]); the size of the FOD is also inversely proportional to the magnitude of the response function used for deconvolution[70]:

$$FOD * RF = DWI \qquad FOD = DWI *^{-1} RF \qquad (1)$$

('*RF*': response function; '*': convolution operation; '$*^{-1}$': deconvolution operation)

Enabling direct comparison of this measure across subjects therefore necessitates *global inter-subject intensity normalisation*, in order for AFD to be minimally influenced by nuisance variables. This typically includes B1 bias field correction, scaling of DWI intensities to a common intensity value according to some representative image statistic (e.g. mean *b*=0 magnitude in white matter), and use of a group average response function for deconvolution[70]: these together ensure that 'one unit of AFD' is comparable across subjects, rather than being defined relative to subject-specific parameters (e.g. coil loading, scanner receiver gain, subject-specific response function magnitudes).

In a similar manner, quantitative analysis of FBC requires inter-subject *connection density normalisation*: that is, if we quantify the intra-axonal cross-sectional area of a particular pathway (e.g. edge of a connectome) across multiple subjects, we want these quantities to be directly comparable across subjects, without being biased by confounding factors that destroy the physical interpretation of this measure or introduce substantial correlations with nuisance reconstruction parameters.

In the brief history of diffusion MRI tractography connectomics, this normalisation has most commonly been achieved by simply generating *the same number of streamlines* for each subject. Or, expressed in an alternative way: if half as many streamlines were generated for one subject as there were for all other subjects, it would seem intuitively logical that the streamline counts in each edge for that subject should be doubled in order for the raw values stored in the connectome matrices to be comparable to other subjects. While generation of an identical number of streamlines across subjects may seem incontrovertible, it is in fact an *imperfect solution* to connection density normalisation. By using a fixed number of streamlines per subject, each streamline effectively represents a *fixed, subject-specific fraction of the total white matter fibre connectivity*. While comparing such quantitative measures across subjects is acceptable as long as they are properly interpreted as such, this metric fails to take into account a number of factors that may differ between subjects that may correspondingly introduce biases or unwanted variance into such an analysis; this includes both biological differences (e.g. widespread reductions in FD) and features of the tractogram reconstructions (e.g. differences in streamline lengths). For a genuine quantitative comparison of *absolute* fibre connection densities between subjects, greater care must therefore be taken.

Here, we demonstrate our recommendation for how this normalisation should be achieved when using specifically the model underlying the 'SIFT'[19] and 'SIFT2'[22] methods, which is itself directly dependent on the AFD measure. Use of alternative reconstruction techniques (in terms of either the underlying diffusion model or alternative semi-global tractography methods) would require that appropriate comparable steps be taken.

The SIFT model defines the *proportionality coefficient* μ_i for subject *i*, which relates the global sum of track density (*TD*) to the global sum of estimated *FD* in the single-subject reconstruction, computed across all fixels *f* in that subject:

$$\mu_i = \frac{\sum_{f \in i} FD_f}{\sum_{f \in i} TD_f} \qquad (2)$$

(For simplicity, the influence of the processing mask within the SIFT model[19] is omitted here.)

In the original SIFT method, this parameter permits direct comparison between the streamlines density and fibre volume within each fixel, in order to drive the streamlines filtering process. In SIFT2, it approximately centres the distribution of streamlines weights about unity. Note that all parameters within this expression are *subject-specific*.

As *FD* is a measure of volume (dimensions L^3) and *TD* is a sum of streamline lengths (dimensions *L*), μ is a measure of *cross-sectional area*, with dimensions L^2. For every streamline, this parameter (multiplied by the weight assigned to that streamline in the case of SIFT2) is a measure of the intra-axonal cross-sectional area represented by that streamline. For each voxel traversed by the streamline, the *product* of this cross-sectional area with the *length* of the streamline intersection *within that voxel* produces the fibre volume contributed to that fixel by that particular streamline within the model.

In the context of FBC quantification, we are interested not in these fixel-wise fibre volumes, but the connection densities of specific macroscopic pathways of interest. Any such pathway is represented as a subset of streamlines in the whole-brain tractogram. For an example

pathway *p* (which is reconstructed by a subset of streamlines *s*), it is the *sum of intra-axonal cross-sectional areas* of the streamlines within that pathway that gives a measure of the intra-axonal cross-sectional area of the pathway $FBC_{p,i}$:

$$FBC_{p,i} = \mu_i \cdot \sum_{s_i \in p} W_{s_i} \quad (3)$$

For subject *i*, the connection density $FBC_{p,i}$ of pathway *p* is the product of the subject-specific proportionality coefficient μ_i and the sum of streamline weights w_i of those streamlines s_i belonging to pathway *p*.

(Note that in the original SIFT method, $w_s = 1$ for all retained streamlines after filtering, but μ_i is modulated during the filtering process.)

This equation suggests that if one wants to compare FBC across subjects (whether for an individual bundle of interest or an entire connectome matrix), simply multiplying the sum of bundle streamlines weights by μ_i is sufficient to produce a measure of FBC that can be compared across subjects. However, parameter μ_i only considers the fibre densities and track densities *within a single subject*; in order to compare these quantities between subjects, we must ensure that parameter μ_i is adjusted appropriately to account for *between-subject variation*, by ensuring that the *fundamental scaling* underlying this parameter is equivalent between subjects.

We can extend Equation (2) as follows:

$$\mu_{i,adj} = \frac{AFD_{ref}}{DWI_{ref}} \cdot |x||y||z| \cdot \frac{\sum_{f \in i} FD_f}{\sum_{f \in i} TD_f} \quad (4)$$

- $\mu_{i,adj}$ is the proportionality coefficient of subject *i* 'adjusted' for facilitation of inter-subject comparison;
- The first term, $\frac{AFD_{ref}}{DWI_{ref}}$, is specific to the spherical deconvolution model if processing were to be performed independently for each subject. It relates to the global scaling of AFD magnitudes within that subject, which is dependent on the magnitude of the diffusion-weighted signal (DWI_{ref}) and the size of the response function for deconvolution that forms the reference unit of AFD (AFD_{ref}).
- The second term, $|x||y||z|$, is the volume of each voxel in the image. This multiplier converts AFD (or fibre volume fractions from a partial volume-based diffusion model) into estimated intra-axonal volumes in mm^3, thereby appropriately scaling connectivity estimates in cases where the DWI voxel size differs across subjects (this also coincidentally gives $\mu_{i,adj}$ and hence FBC, units of mm^2).
- In the specific case of the SIFT model, no term relating to the inter-subject scaling of TD appears in this expression: this is calculated in fixed units of mm regardless of DWI spatial resolution, and therefore cannot vary across subjects (this may, however, not be the case for alternative models or methods).

The global intensity normalisation and group average response function components of the recommended pre-processing pipeline for AFD analysis are tailored to make equivalent across subjects the values of DWI_{ref} and AFD_{ref}, respectively. As such, if this pipeline is followed, the term $\frac{AFD_{ref}}{DWI_{ref}}$ is identical across subjects by construction, and simply multiplying the sum of streamline weights within a pathway of interest (e.g. a connectome edge) by μ_i permits direct quantitative comparison of FBC between subjects, in a manner that appropriately accounts for many variables that would otherwise confound the interpretation of streamline counts as 'connection density'.

The consequences of this connection density normalisation are demonstrated in Figure 13. This demonstration consists of 16 individual synthetic subjects, each of whom possesses a single white matter fibre bundle. The fundamental properties of this bundle — length, width, and microscopic FD per voxel — vary among the subjects; additionally, the number of streamlines seeded in each white matter voxel is also varied. The lower part of Figure 13 then demonstrates visually how the quantified 'connectivity' of this bundle across the 16 subjects changes in magnitude across the different subjects, depending on the exact measure of 'connectivity' that is utilised. The connectivity measures demonstrated are as follows:

- The macroscopic bundle volume *V*;
- The streamline count *N*;
- The number of streamlines divided by the length of the streamlines[41,71];
- The mean *FD* sampled along streamlines within the bundle;
- *FBC*, incorporating the proposed connection density normalisation.

We assert that the proposed connection density normalisation (highlighted in green in Figure 13) is most appropriate for quantitative comparison of endpoint-to-endpoint connectivity across subjects; it matches the theoretical properties of the FBC metric:

- *Scales* with the cross-sectional area of the bundle;
- *Scales* with the underlying FD in each voxel;
- *Does not scale* with the length of the bundle;
- *Does not scale* with the number of streamlines generated.

DISCUSSION

As stated in the 'Introduction' section, the information presented in the 'Methods' section is intended to serve two principal purposes:

1. To properly contextualise a class of methods already present in the literature that perform tractogram

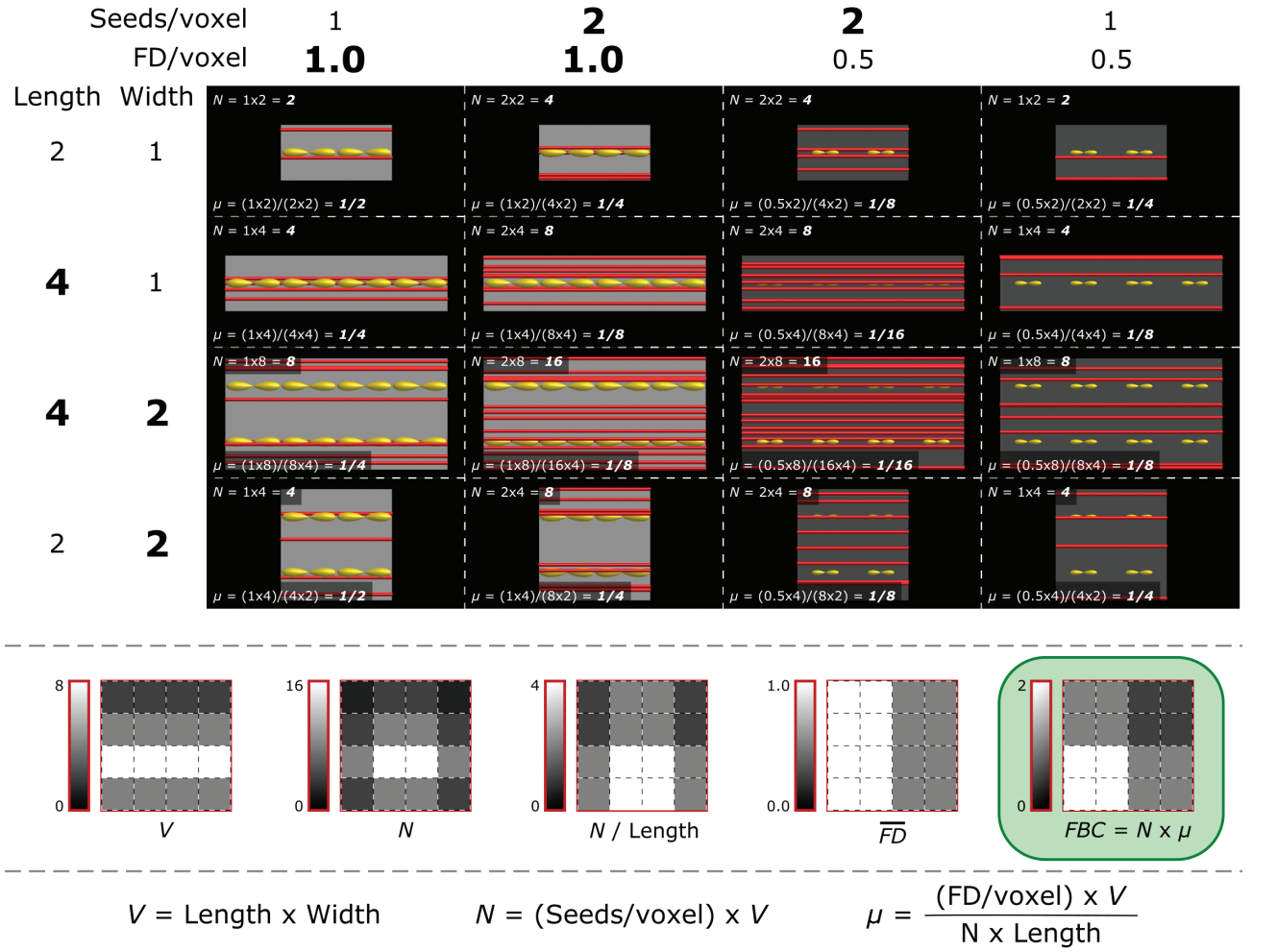

Fig. 13. Demonstration of the efficacy of the proposed inter-subject connection density normalisation. Each of the 16 panels represents a synthetic subject, containing one white matter bundle reconstructed by streamlines. For each, the number of streamlines generated N, and the 'proportionality coefficient' μ within the SIFT model (derived from Equation 2), are provided. The matrix representations at the bottom show visually the relative connection densities quantified for the different bundles, for various 'connectivity' metrics of interest: volume of bundle V; number of streamlines N; number of streamlines divided by the streamline length; the mean fibre density (FD) sampled along streamlines within the bundle; the proposed fibre bundle capacity (FBC) measure incorporating connection density normalisation (highlighted in green).

manipulation for the purposes of quantitative tractography by elucidating:

a. Why these methods are designed the way they are (see also 'Relationship to existing methods' section);
b. That many 'alternative' methods for white matter connectivity analysis frequently suggested informally by community members have already been considered, but have specific weaknesses compared to established methods;
c. That the goal of 'quantifying bundle connectivity' is in fact accessible using these existing methods (while of course acknowledging all of the limitations of such methods and other components of the analysis pipeline).

- To demonstrate how to appropriately extend the application of these methods from the correct estimation of relative connection strengths of different bundles *within* a single individual to estimation of relative connection strengths of a bundle *across* individuals (Figure 13).

Relationship to existing methods

In 'Algorithm 4: "Optimizsed streamline weights"', the fact that the existing SIFT2 algorithm operates on the same mechanism as that arrived at through the course of logic presented is not coincidental. Here, we note that there are a number of other existing methods that also operate similarly:

- The 'linear fascicle evaluation (LiFE)'[21] and 'convex optimisation modelling for microstructure-informed tractography (COMMIT)'[20] methods both operate on an identical premise — modulating the weight of contributions from individual streamlines within the tractogram,

in such a way that the streamlines densities are faithful to the underlying image information — except that they operate directly on the diffusion image data, as explained in the 'Comparing tractograms and image data' section.
- The earlier 'BlueMatter',[18] 'MicroTrack',[72] and 'SIFT'[19] methods also lie within this classification: while these algorithms instead *select a subset of streamlines* that together produce a faithful representation of the image data, this is mathematically equivalent to setting the contribution weights of those streamlines omitted from the tractogram to zero.
- Another method entitled 'global tractography with embedded anatomical priors'[73] optimises streamline weights based on a tractogram initially constructed using streamlines tractography, but also optimises other features of the reconstruction (such as streamlines trajectories) based on the diffusion image data in a manner more similar to genuinely global tractography algorithms.

It has been shown that utilisation of such methods yields white matter connectivity estimates with properties that are more faithful to biological reality[44] and that their influence on network connectivity analyses is non-negligible.[41] Such methods are publicly accessible and have already been adopted in some studies in the neuroscience research literature.[74–87]

Qualifying the 'FBC' metric

The origins and biological significance of the FBC metric require explicit communication, as it is a frequent source of confusion.

- It should be noted that the quantification of specifically *total intra-axonal cross-sectional area* is in part a direct consequence of the proportionality of the diffusion MRI signal (under certain conditions) to the *local intra-axonal volume* of fibre bundles,[70] in conjunction with the spatial/orientation information of the tractogram reconstruction. It is not a metric that was devised in isolation, with methods then developed to quantify such, but a natural consequence of what *can be quantified* given the data available.
- Where there is heterogeneity in axon diameters, the FBC metric will not be a proportional estimate of axon *count*, as was proposed for simplicity in the 'Metric of "connectivity"' section. The influence of heterogeneity in axon diameters can be considered as follows. For a given fixed value of FBC, there could be many axons of small diameter or few axons of larger diameter. In the latter case, while there are fewer connections, conduction velocity will be greater, as will be the potential firing rate.[88] As such, when seeking a *univariate* quantification of 'connectivity', which specifically relates to the capacity for information transmission, this metric exhibits somewhat desirable behaviour in the presence of such heterogeneity, at least within the limitations of expressing such as a single scalar quantity. It should also be noted that conventionally acquired diffusion-weighted image data are unable to resolve differences in axon diameter[89,90] — indeed even state-of-the-art acquisitions and hardware struggle to resolve such in the presence of crossing fibres[91–93] — so overcoming this limitation in specificity is non-trivial.
- While the presence of myelin does influence the conduction of action potentials, conventionally acquired diffusion MRI data are relatively insensitive to the presence or absence of such.[94]
- This metric is intentionally *not* proportional to length, unlike bundle volume. Although bundle length may alter axon conduction delays,[95] we consider such to be an independent property of white matter connections that does not directly influence the notion of 'bandwidth'.
- Unlike *macroscopic* bundle volume (or indeed cross-sectional area), this metric additionally considers the density of axonal packing within the white matter traversed.

The prevalence of studies utilising quantitative metrics of white matter bundles such as streamline count or bundle volume highlight the demand for an appropriate quantification of 'connectivity' of white matter bundles. We posit that, compared to other univariate metrics already in use in the community, the FBC metric is in fact *more faithful* to a subjective notion of 'connectivity', based on both the logic presented above and the evidence shown in Figure 13.

Whole-brain tractography is compulsory

With the exception of Algorithm 1, all other algorithms described here necessitate the use of a whole-brain tractogram reconstruction, even in the scenario where it is only the connectivity of one specific white matter bundle that is of interest. This includes the SIFT2 algorithm shown as Algorithm 4, and similar methods described above in the 'Relationship to existing methods' section. The reason for this is as demonstrated in Figure 8 in relation to Algorithm 1. If a white matter bundle (as defined as a set of streamlines that is *not* a whole-brain tractogram) is interpreted in isolation, then *anywhere* there exists a voxel that contains collinear fibres *not* belonging to that bundle, such a quantification will erroneously attribute the entire FD in that orientation to that bundle. Given the contrast between the complexity of white matter bundle trajectory/shape and the fixed lattice of an image voxel grid, this will *always* occur. Note that this is an issue regardless of whether or not any adjacent bundle sharing that voxel is or is not also 'of interest' experimentally.

The functionality afforded by the use of a whole-brain tractogram — whether very directly and explicitly in the case of Algorithm 2, or more indirectly/implicitly in other algorithms — is to determine the fraction of the fibre volume within each fixel that should be attributed to the bundle of interest, in order to prevent the over-attribution of FD that occurs in Algorithm 1. As such, we here recapitulate a message crucial to prevent further erroneous use of these methods in the community:

> Semi-global methods *must be applied to a whole-brain tractogram*, with interrogation of bundles of interest performed after the fact (as shown in Algorithm 4).

If this condition is *not* satisfied, then when interrogating discrepancies between streamlines density and FD, such algorithms are unable to distinguish between differences that arise due to tractogram reconstruction biases and differences that arise due to the presence of biological fibre pathways that contribute to the diffusion-weighted signal but are absent from the streamlines reconstruction due to erroneous prior removal (see Figure 8). Note that this description deliberately does not exclude the prospect of tractogram manipulation in between whole-brain fibre-tracking and semi-global algorithm application — for instance, one could envisage that some approach for data-driven classification and removal of false-positive streamlines could be applied in between these steps — but it is vital that the tractogram provided to a semi-global optimisation process comprehensively cover the domain of plausible fibre trajectories within the imaged region, as such a comprehensive set is necessary for explaining the diffusion-weighted signal.

Alternatives for connection density normalisation

A common idea in applications of white matter tractography, particularly in the construction of the structural connectome, is that there is a range of other parameters that should be applied as multiplicative factors to connectivity measures, in order to 'compensate' for variations in those parameters that may indirectly influence the results of streamlines tractography or connectome construction. Here, we take the opportunity to clarify a few concepts that have arisen in our own communications on the topic.

Number of streamlines in the connectome

Although it is trivial to use a fixed number of streamlines for tractogram construction across subjects for the implicit purpose of connection density normalisation, typically the proportion of those streamlines successfully assigned to a pair of parcels (and that hence contribute to the connectome) will vary between subjects,[96] due to a range of factors; note that this still occurs even with the controlled termination of streamlines such as in anatomically constrained tractography (ACT),[16] though technical improvements can reduce this variance.[97,98] While it is tempting to normalise the connectome edge values by scaling for the number of streamlines in the *connectome* (rather than using the number of streamlines in the *tractogram* as reference) to 'compensate' for this inter-subject discrepancy, it is also entirely possible for differences in this parameter to be reflective of a *genuine effect of interest*.

For instance, consider the case where a large tumour within the white matter in one hemisphere results in a substantial number of streamlines terminating within that tumour, rather than reaching some alternative grey matter target. If the subject-specific tumour *does not appear as a node* within the connectome parcellation, and the total number of streamlines generated across subjects is equivalent, then the total number of streamlines *in the connectome* for this particular subject would be decreased relative to other subjects (as the total number of streamlines is the same, but the fraction of those assigned to the connectome is reduced). A useful interpretation here is to treat the tumour as a 'latent connectome node'. Consider the situation if the tumour were to be segmented and included in the connectome parcellation, with streamlines terminating within that node and being assigned as such; but following connectome construction, that node would then be *erased* from the connectome matrix. We now consider two options for normalisation:

1. If a fixed number of streamlines in the *tractogram* per subject were to be used, then the subject with the tumour would have a reduced total connection density within the connectome, particularly within bundles affected by the tumour, which is likely to be at least somewhat faithful to biological reality.
2. If instead the connectomes were scaled based on the number of streamlines in the *connectome* in each subject (bearing in mind that this scaling would by necessity occur *after* removal of the tumour node if the total connection density is to be equivalent across subjects), the connection densities of *all* pathways in that subject would be *increased* as a consequence of that process. This would be *misleading*, as it would suggest that all white matter bundles not affected by the tumour in that subject have *increased connectivity* in that subject relative to healthy controls.

The important observation here is that while the number of streamlines in the *tractogram reconstruction* may not be equal to the number of streamlines in the *connectome* (and this ratio may vary across participants) and this effect *can* be influenced by inadequacies in data processing and reconstruction,[96] this is not the *only* source of such mismatch and should therefore be interpreted with caution. For instance, consider the influence of the reconstructed corticospinal tract, where streamlines exit the inferior edge of the image data via the spinal column.

If no connectome parcel is explicitly defined at this location, then these streamlines will not contribute to the connectome, despite the known anatomical validity of this bundle and its non-negligible contribution to the diffusion-weighted signal. Variance in the density of this bundle across subjects could therefore manifest as differences in streamline count within connectomes across subjects; the latter would not ideally be interpreted as either indicative of a difference in reconstruction efficacy, or a 'nuisance' effect between individuals,

Intracranial/brain/white matter volume

Another concept commonly raised in the discussion on this topic is that: if subject brains vary considerably in physical size, but the same number of streamlines is generated for each, then a comparison of streamlines density between them *must* be biased, as each individual streamline reconstructed in a physically larger brain likely represents a larger density of biological fibres than does each individual streamline reconstructed in a physically smaller brain. Users of such methods correspondingly often propose *dividing all estimates of connectivity* by the estimated intracranial/brain/white matter volume of that subject, as a 'correction' for this effect. There are a number of comments to be made on this concept:

- It pre-supposes that if the cross-sectional area of a bundle scales directly in proportion to brain size, then that bundle should be reported as possessing equivalent 'connectivity' between brains of different sizes; this is the *intent* of such scaling and so should be appreciated as such.
- There is an implicit assumption in this proposal that, even between the largest and smallest of brains, the voxel-wise FD within the white matter is equivalent; this is, however, not guaranteed to be the case.
- Performing scaling as proposed in the 'Inter-subject connection density normalizsation' section intrinsically handles this confound in an appropriate fashion. A larger brain will likely have more white matter voxels and therefore a larger FD sum, but it will also have a greater sum of streamline lengths. Consequently, while FBC may be greater in a large brain than in a small brain if the bundle size scales in direct proportion to brain size, this would not be an unwanted confound of brain size, but a realistic measurement of a greater information-carrying capacity of that fibre bundle in the larger brain.
- The *interpretation* of experimental outcomes also changes by necessity through such scaling. For instance, if one were to compare the connection density of a specific bundle of interest between two groups, where this brain volume scaling factor were applied to the connectivity estimates prior to the comparison, then the actual hypothesis being tested would be 'the connection-density-divided-by-white-matter-volume of this pathway is not equivalent between two groups'.

We instead suggest that intracranial/brain volume (and other such regressors) may be better handled as *nuisance parameters* when performing statistical testing. In this way, the hypothesis being tested would better reflect the intention of the experiment, for example, 'the connection density of this pathway is not equivalent between the two groups, the magnitude of which cannot be attributed to differences in brain volume alone'.

The effect of inter-node distance in streamlines tractography

The relationship between white matter pathway length and estimated connection density has attracted considerable interest in this field.[19,41,71] There are, however, *multiple mechanisms* by which pathway length may influence streamlines-based connectivity; and in our experience these are regularly conflated or confused. We therefore take this opportunity to disambiguate the effects of which we are aware.

Most frequently, discussion regarding bundle length biases are in reference to the effect arising from homogeneous seeding throughout the white matter: because longer pathways present a greater volume in which streamline seeds may be drawn, they will typically be reconstructed by a greater number of streamlines than shorter pathways. A naïve direct correction of this seeding density effect is to make the contribution of each streamline to the connectome the reciprocal of its length[71]; this has been shown to be incomplete, as the graph theory metrics derived from connectomes calculated in such a manner differ significantly from those produced using more comprehensive data-driven correction of fibre tracking biases.[41]

A distinctly different effect is attributed to probabilistic streamlines algorithms. Due to the spatial dispersion of streamlines when using a probabilistic tracking algorithm, biologically connected nodes that are distant from one another are likely to have a reduced reconstructed connection density: streamlines emanating from one parcel increasingly disperse from one another as a function of distance from that parcel, such that the fraction of those streamlines reaching the intended target decreases as a function of distance.[1] This effect is, however, not a bias that can be corrected naïvely. For instance, consider two distant nodes that are *not* connected biologically, yet their immediate spatial neighbouring parcels *are* connected biologically, and therefore there is a plausible white matter pathway between them. The connectivity estimated between these two nodes using a probabilistic streamlines algorithm will be *increased* by this probabilistic dispersion effect relative to if the white matter pathway were short. Data regarding inter-node

1 We note that *deterministic* streamlines algorithms do *not* solve the issue described here. With such methods, instead of the fraction of streamlines reaching the intended target decreasing smoothly as a function of distance, the likelihood of a dichotomous switch from all true connections to all false connections increases as a function of distance.

distances alone are therefore not sufficient to 'correct' for this effect.

We propose that this particular effect is better understood as a *distance-dependent connectome blurring:* biologically strong connections are 'spread out' in the reconstruction to edges corresponding to spatially adjacent nodes, with the extent of that blurring being a function of the pathway length. The way in which fibre orientation uncertainty/dispersion is modelled and utilised in the tractography algorithm is likely to influence the magnitude of this effect. While there exists a tailored correction mechanism for addressing this specific issue in the context of targeted tracking when quantifying a *probability* of connectivity,[99] to our knowledge there has been no such mechanism proposed for addressing this issue when quantifying the *density* of white matter connections.

We further clarify that there is another streamlines tractography effect that bears similarity to that described above, but behaves slightly differently and applies to both deterministic and probabilistic streamlines algorithms. Opportunities for the streamlines algorithm to sample from an inappropriate fibre orientation (particularly in the presence of crossing fibres), and therefore construct a wholly erroneous trajectory, increase as a function of bundle length. This effect has also to our knowledge not been investigated comprehensively but should be considered as distinct from both other 'influences of bundle length on streamline count' described above.

Relationship to fixel-based analysis metrics

We have recently published on the disentanglement of statistical effects in microscopic FD and macroscopic changes in cross-sectional area, made possible within the FBA framework.[69] Due to the subsequent interest we received in the potential incorporation of such fixel-wise measures into tractogram and/or structural connectome quantification, here we clarify the relationship between these fixel-wise measures and FBC.

For any particular white matter pathway in the brain, FBC quantified using a global or semi-global tractography approach will scale directly proportionally with *both* the microscopic FD (resulting in a greater number of streamlines or increased streamlines weights traversing any particular fixel) *and* the macroscopic pathway cross-sectional area (resulting in a greater breadth of fixels traversed by the streamlines within that pathway, and hence likely also more streamlines being assigned to that pathway), as shown in Figure 13. FBC quantified in this manner therefore behaves most comparably to the 'fibre density and bundle cross-section (FDC)' measure[69]; but crucially, FBC is quantified as an endpoint-to-endpoint connectivity measure, whereas FDC is a local fixel-wise quantitative measure (as shown in Figure 3).

There is an additional clarification required regarding terminology between these two cases:

- In FBA, the 'fibre bundle cross-section (FC)' metric is in fact a *change in the cross-sectional area*; in the calculation of the FDC metric, this is used to *modulate* the local quantitative measure;
- In tractogram-based connectivity quantification, FBC of any particular pathway is typically *directly proportional* to the *absolute* bundle cross-sectional area.

Another concept frequently raised in communications in this context is the prospect of an alternative quantitative metric for connectome construction, which exploits the quantitative nature of these per-fixel metrics. That is, instead of *summing streamlines weights* within a pathway (as an estimate of intra-axonal cross-sectional area), quantitative values from some metric of interest are instead *sampled along the corresponding streamlines trajectories*. This could conceivably be done in one of two ways, shown as Algorithms 5a and 5b in Figure 14:

a. From the set of streamlines constituting a pathway of interest/connectome edge, derive a mask corresponding to the areas (either voxels or fixels) in which the values of the quantitative metric should be sampled; some statistic from these elements (e.g. the mean) is then calculated to produce a single scalar value per connectome edge.
b. For each streamline, measure the value of the metric at every point along the streamline trajectory; calculate some statistic from the samples along each streamline (e.g. the mean) in order to produce a single scalar value per streamline; calculate some statistic from these per-streamline values (e.g. the mean) to produce a single scalar value per connectome edge.

The *intent* behind such suggestions is that these quantities would exhibit a reduced influence from the errors and biases associated with streamlines tractography compared to the FBC metric, would incorporate the quantitative nature of those underlying metrics, and would inherit the fixel specificity of the FBA metrics (there are already many applications that have utilised such sampling along streamline trajectories but in conjunction with voxel-wise imaging metrics). Such quantification should, however, be interpreted in accordance with the relevant calculations. For instance, calculating the mean of the FD metric along a pathway using one of the two approaches discussed previously provides a measure that could be interpreted as 'mean intra-axonal volume fraction within the bundle'; which, while potentially informative, would not be an *absolute* measure of bundle connectivity, as it neither scales with bundle width (Figure 13), nor does it consider partial volume with other bundles (as demonstrated in Algorithm 1, Figures 7 and 8).

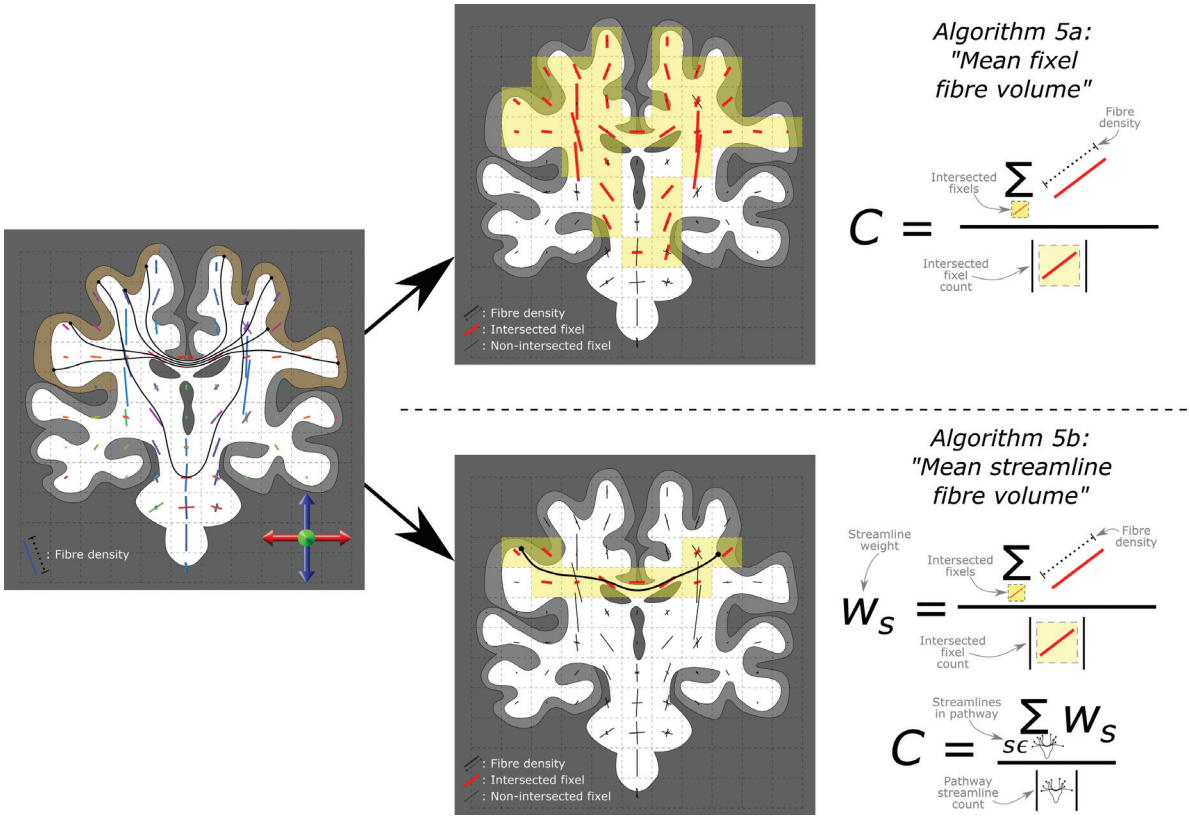

Fig. 14. Visual demonstration of the operation of hypothetical alternative Algorithms 5a and 5b. (a) For the pathway of interest (left panel; streamlines), derive a mask of fixels traversed (top panel; red fixels within yellow voxels). Within this mask, compute from the fibre densities of those fixels (encoded visually as fixel lengths) the mean (equation at right shows the sum of fixel fibre densities divided by the number of traversed fixels), as a measure of 'connectivity' *C* of the pathway. (b) For each individual streamline within the pathway of interest (left panel), derive a mask of fixels traversed by that streamline (bottom panel; red fixels). Across those fixels, compute the mean fibre density (first equation at right shows the sum of traversed fixel fibre densities divided by the number of fixels traversed by that streamline). Finally, take the mean of these values across the streamlines corresponding to the pathway of interest (second equation at right shows sum of streamline weights divided by the number of streamlines) as a measure of 'connectivity' *C* of the pathway.

Software implementations

The algorithms described in the section 'The algorithmic basis of quantitative streamlines tractography' have been made available as part of the *MRtrix3* software package[100] (www.mrtrix.org; command and option names as at version 3.0.0):

- Algorithm 1, 'Fixel mask': afdconnectivity;
- Algorithm 2, 'Weighted fixel mask': afdconnectivity using the -wbft option;
- Algorithm 3, 'Volume-averaged streamline weights': tcksift2 using the -linear option;
- Algorithm 4, 'Optimised streamline weights': tcksift2.

The SIFT method[19] mentioned in the 'Relationship to existing methods' section is additionally available as command tcksift.

CONCLUSION

We have shown how the algorithmic design of a class of 'semi-global' tractogram optimisation algorithms is the inevitable result of trying to incorporate global image information into otherwise locally greedy, streamlines-based tractography data. When used appropriately, these methods address one of the major fundamental technical limitations in the field that otherwise precludes the direct comparison of quantitative estimates of white matter connection density between subjects. We hope that the explanations and clarifications contained herein assist those readers for whom the purpose (or indeed existence) of these approaches was unclear.

ACKNOWLEDGEMENTS

We are grateful to the National Health and Medical Research Council (NHMRC) of Australia and the Victorian Government's Operational Infrastructure Support Program for their support.

RS is supported by fellowship funding from the National Imaging Facility (NIF), an Australian Government National Collaborative Research Infrastructure Strategy (NCRIS) capability.

JDT was supported with funding from the European Research Council under the European Union's Seventh Framework Programme [FP7/20072013], ERC grant agreement no. [319456] (developing Human Connectome Project) and MRC strategic funds [MR/K006355/1]. JDT was also supported by the Wellcome/EPSRC Centre for Medical Engineering at King's College London [WT 203148/Z/16/Z] and by the National Institute for Health Research (NIHR) Biomedical Research Centre at Guy's and St Thomas' NHS Foundation Trust and King's College London. The views expressed are those of the authors and not necessarily those of the NHS, the NIHR, or the Department of Health.

REFERENCES

1. Mori S, van Zijl PCM. Fiber tracking: Principles and strategies – a technical review. *NMR in Biomedicine*. 2002;15(7–8):468–480.
2. Dell'acqua F, Catani M. Structural human brain networks: Hot topics in diffusion tractography. *Current Opinions in Neurology*. 2012;25(4):375–383.
3. Johansen-Berg H, Behrens TEJ. Just pretty pictures? What diffusion tractography can add in clinical neuroscience. *Current Opinion in Neurology*. 2006;19(4):379–385.
4. Griffa A, Baumann PS, Thiran J-P, Hagmann P. Structural connectomics in brain diseases. *Mapping the Connectome*. 2013;80(0):515–526.
5. Tournier J-D, Mori S, Leemans A. Diffusion tensor imaging and beyond. *Magnetic Resonance in Medicine*. 2011;65(6):1532–1556.
6. Mori S, Crain BJ, Chacko VP, van Zijl PCM. Three-dimensional tracking of axonal projections in the brain by magnetic resonance imaging. *Annals of Neurology*. 1999;45(2):265–269. doi:10.1002/1531-8249(199902)45:2%3C265::aid-ana21%3E3.0.co;2-3
7. Conturo TE, Lori NF, Cull TS, et al. Tracking neuronal fiber pathways in the living human brain. *Proceedings of the National Academy of Sciences of the United States of America*. 1999;96(18):10422–10427.
8. Basser PJ, Pajevic S, Pierpaoli C, Duda J, Aldroubi A. In vivo fiber tractography using DT-MRI data. *Magnetic Resonance in Medicine*. 2000;44(4):625–632.
9. Jeurissen B, Descoteaux M, Mori S, Leemans A. Diffusion MRI fiber tractography of the brain. *NMR in Biomedicine*. 2017;32:e3785.
10. Jones DK, Knösche TR, Turner R. White matter integrity, fiber count, and other fallacies: The do's and don'ts of diffusion MRI. *NeuroImage*. 2013;73(0):239–254.
11. Mangin J-F, Poupon C, Cointepas Y, et al. A framework based on spin glass models for the inference of anatomical connectivity from diffusion-weighted MR data – a technical review. *NMR in Biomedicine*. 2002;15(7–8):481–492.
12. Kreher BW, Mader I, Kiselev VG. Gibbs tracking: A novel approach for the reconstruction of neuronal pathways. *Magnetic Resonance in Medicine*. 2008;60(4):953–963.
13. Reisert M, Mader I, Anastasopoulos C, Weigel M, Schnell S, Kiselev V. Global fiber reconstruction becomes practical. *NeuroImage*. 2011;54(2):955–962.
14. Mangin J-F, Fillard P, Cointepas Y, Le Bihan D, Frouin V, Poupon C. Toward global tractography. *Mapping the Connectome*. 2013;80(0):290–296.
15. Christiaens D, Reisert M, Dhollander T, Sunaert S, Suetens P, Maes F. Global tractography of multi-shell diffusion-weighted imaging data using a multi-tissue model. *NeuroImage*. 2015;123:89–101.
16. Smith RE, Tournier J-D, Calamante F, Connelly A. Anatomically-constrained tractography: Improved diffusion MRI streamlines tractography through effective use of anatomical information. *NeuroImage*. 2012;62(3):1924–1938.
17. Girard G, Descoteaux M. Anatomical tissue probability priors for tractography. *CDMRI*. 2012:174–185. https://www.researchgate.net/publication/237170488_Anatomical_tissue_probability_priors_for_tractography
18. Sherbondy AJ, Dougherty RF, Ananthanarayanan R, Modha DS, Wandell BA. Think Global, Act Local; Projectome estimation with BlueMatter. *Medical Image Computing and Computer-Assisted Intervention*. 2009;12:861–868. https://www.ncbi.nlm.nih.gov/pmc/articles/PMC3076280/
19. Smith RE, Tournier J-D, Calamante F, Connelly A. SIFT: Spherical-deconvolution informed filtering of tractograms. *NeuroImage*. 2013;67(0):298–312.
20. Daducci A, Dal Palú A, Lemkaddem A, Thiran J. COMMIT: Convex optimization modeling for micro-structure informed tractography. *IEEE Transactions on Medical Imaging*. 2014;34:246–257. doi:10.1109/TMI.2014.2352414
21. Pestilli F, Yeatman JD, Rokem A, Kay KN, Wandell BA. Evaluation and statistical inference for human connectomes. *Nature Methods*. 2014;11(10):1058–1063.
22. Smith RE, Tournier J-D, Calamante F, Connelly A. SIFT2: Enabling dense quantitative assessment of brain white matter connectivity using streamlines tractography. *NeuroImage*. 2015;119:338–351.
23. Sporns O, Tononi G, Kötter R. The human connectome: A structural description of the human brain. *PLoS Computational Biology*. 2005;1(4):e42.
24. Hagmann P. From diffusion MRI to brain connectomics. 2005. doi:10.5075/epfl-thesis-3230
25. Christiaens D, Tournier JD. Chapter 20 – Modeling fiber orientations using diffusion MRI. In: Seiberlich N, Gulani V, Calamante F, et al., eds. *Advances in Magnetic Resonance Technology and Applications*. Vol 1. Quantitative Magnetic Resonance Imaging. Academic Press; 2020:509–532. doi:10.1016/B978-0-12-817057-1.00022-6
26. Smith RE, Connelly A, Calamante F. Chapter 21 – Diffusion MRI fiber tractography. In: Seiberlich N, Gulani V, Calamante F, et al., eds. *Advances in Magnetic Resonance Technology and Applications*. Vol 1. Quantitative Magnetic Resonance Imaging. Academic Press; 2020:533–569. doi:10.1016/B978-0-12-817057-1.00023-8
27. Calamante F. The seven deadly sins of measuring brain structural connectivity using diffusion MRI streamlines fibre-tracking. *Diagnostics*. 2019;9(3):115. doi:10.3390/diagnostics9030115
28. Le Bihan D, Johansen-Berg H. Diffusion MRI at 25: Exploring brain tissue structure and function. *Neuroimaging: Then, Now and the Future*. 2012;61(2):324–341.
29. Sotiropoulos SN, Zalesky A. Building connectomes using diffusion MRI: Why, how and but. *NMR in Biomedicine*. 2019;32(4):e3752. doi:10.1002/nbm.3752
30. Yeh C-H, Jones DK, Liang X, Descoteaux M, Connelly A. Mapping structural connectivity using diffusion MRI: Challenges and opportunities. *Journal of Magnetic Resonance Imaging*. doi:10.1002/jmri.27188
31. Tournier J-D, Calamante F, Connelly A. Robust determination of the fibre orientation distribution in diffusion MRI: Non-negativity constrained super-resolved spherical deconvolution. *NeuroImage*. 2007;35(4):1459–1472.
32. Derek K. Jones PD. *Diffusion MRI: Theory, Methods, and Applications*. Oxford University Press; 2011. http://books.google.com.au/books?id=dbZCMePD52AC
33. Johansen-Berg H, Behrens TEJ. *Diffusion MRI: From Quantitative Measurement to In-Vivo Neuroanatomy*. Academic Press; 2009. http://books.google.com.au/books?id=N20nnxByjVAC
34. Chamberland M, Raven EP, Genc S, et al. Dimensionality reduction of diffusion MRI measures for improved tractometry of the human brain. *NeuroImage*. 2019;200:89–100. doi:10.1016/j.neuroimage.2019.06.020
35. Jones D, Travis A, Eden G, Pierpaoli C, Basser P. PASTA: Pointwise assessment of streamline tractography attributes. *Magnetic Resonance in Medicine*. 2005;53(6):1462–1467.
36. Yeatman JD, Dougherty RF, Myall NJ, Wandell BA, Feldman HM. Tract profiles of white matter properties: Automating fiber-tract quantification. *PLoS ONE*. 2012;7(11):e49790.
37. Corouge I, Fletcher PT, Joshi S, Gouttard S, Gerig G. Fiber tract-oriented statistics for quantitative diffusion tensor MRI analysis. *Medical Image Analysis*. 2006;10(5):786–798. doi:10.1016/j.media.2006.07.003
38. Colby JB, Soderberg L, Lebel C, Dinov ID, Thompson PM, Sowell ER. Along-tract statistics allow for enhanced tractography analysis. *NeuroImage*. 2012;59(4):3227–3242.
39. Dayan M, Monohan E, Pandya S, et al. Profilometry: A new statistical framework for the characterization of white matter pathways, with application to multiple sclerosis. *Human Brain Mapping*. 2016;37(3):989–1004. doi:10.1002/hbm.23082
40. Fornito A, Zalesky A, Breakspear M. Graph analysis of the human connectome: Promise, progress, and pitfalls. *Mapping the Connectome*. 2013;80(0):426–444.
41. Yeh C-H, Smith RE, Liang X, Calamante F, Connelly A. Correction for diffusion MRI fibre tracking biases: The consequences for structural connectomic metrics. *NeuroImage*. 2016;142:150–162.
42. Rubinov M, Sporns O. Complex network measures of brain connectivity: Uses and interpretations. *Computational Models of the Brain*. 2010;52(3):1059–1069.
43. Sporns O. Network attributes for segregation and integration in the human brain. *Macrocircuits*. 2013;23(2):162–171.

44. Smith RE, Tournier J-D, Calamante F, Connelly A. The effects of SIFT on the reproducibility and biological accuracy of the structural connectome. *NeuroImage*. 2015;104(0):253–265.
45. Savadjiev P, Campbell JSW, Descoteaux M, Deriche R, Pike GB, Siddiqi K. Labeling of ambiguous subvoxel fibre bundle configurations in high angular resolution diffusion MRI. *NeuroImage*. 2008;41(1):58–68.
46. Close TG, Tournier J-D, Johnston LA, Calamante F, Mareels I, Connelly A. Fourier Tract Sampling (FouTS): A framework for improved inference of white matter tracts from diffusion MRI by explicitly modelling tract volume. *NeuroImage*. 2015;120(0):412–427.
47. Daducci A, Dal Palú A, Descoteaux M, Thiran J-P. Microstructure Informed Tractography: Pitfalls and open challenges. *Frontiers in Neuroscience*. 2016;10:247.
48. Girard G, Daducci A, Petit L, et al. AxTract: Toward microstructure informed tractography. *Human Brain Mapping*. 2017;38(11):5485–5500.
49. Raffelt DA, Smith RE, Ridgway GR, et al. Connectivity-based fixel enhancement: Whole-brain statistical analysis of diffusion MRI measures in the presence of crossing fibres. *NeuroImage*. 2015;117:40–55.
50. Behrens TEJ, Woolrich MW, Jenkinson M, et al. Characterization and propagation of uncertainty in diffusion-weighted MR imaging. *Magnetic Resonance in Medicine*. 2003;50(5):1077–1088.
51. Dell'Acqua F, Rizzo G, Scifo P, Clarke RA, Scotti G, Fazio F. A model-based deconvolution approach to solve fiber crossing in diffusion-weighted MR imaging. *IEEE Transactions on Biomedical Engineering*. 2007;54(3):462–472. doi:10.1109/TBME.2006.888830
52. Alexander DC, Hubbard PL, Hall MG, et al. Orientationally invariant indices of axon diameter and density from diffusion MRI. *NeuroImage*. 2010;52(4):1374–1389.
53. Assaf Y, Basser PJ. Composite hindered and restricted model of diffusion (CHARMED) MR imaging of the human brain. *NeuroImage*. 2005;27(1):48–58.
54. Assaf Y, Blumenfeld-Katzir T, Yovel Y, Basser PJ. AxCaliber: A method for measuring axon diameter distribution from diffusion MRI. *Magnetic Resonance in Medicine*. 2008;59(6):1347–1354.
55. Behrens TEJ, Johansen-Berg H, Jbabdi S, Rushworth MFS, Woolrich MW. Probabilistic diffusion tractography with multiple fibre orientations: What can we gain? *NeuroImage*. 2007;34(1):144–155.
56. Kaden E, Kelm ND, Carson RP, Does MD, Alexander DC. Multi-compartment microscopic diffusion imaging. *NeuroImage*. 2016;139:346–359.
57. Panagiotaki E, Schneider T, Siow B, Hall MG, Lythgoe MF, Alexander DC. Compartment models of the diffusion MR signal in brain white matter: A taxonomy and comparison. *NeuroImage*. 2012;59(3):2241–2254.
58. Zhang H, Schneider T, Wheeler-Kingshott CA, Alexander DC. NODDI: Practical – in vivo neurite orientation dispersion and density imaging of the human brain. *NeuroImage*. 2012;61(4):1000–1016.
59. Tournier J-D, Calamante F, Gadian DG, Connelly A. Direct estimation of the fiber orientation density function from diffusion-weighted MRI data using spherical deconvolution. *NeuroImage*. 2004;23(3):1176–1185.
60. Jeurissen B, Tournier J-D, Dhollander T, Connelly A, Sijbers J. Multi-tissue constrained spherical deconvolution for improved analysis of multi-shell diffusion MRI data. *NeuroImage*. 2014;103(0):411–426.
61. Desikan RS, Ségonne F, Fischl B, et al. An automated labeling system for subdividing the human cerebral cortex on MRI scans into gyral based regions of interest. *NeuroImage*. 2006;31(3):968–980.
62. Fischl B. FreeSurfer. *Neuroimage*. 2012;62(2):774–781.
63. Calamante F, Tournier J-D, Jackson GD, Connelly A. Track-density imaging (TDI): Super-resolution white matter imaging using whole-brain track-density mapping. *NeuroImage*. 2010;53(4):1233–1243.
64. Stadlbauer A, Buchfelder M, Salomonowitz E, Ganslandt O. Fiber density mapping of gliomas: Histopathologic evaluation of a diffusion-tensor imaging data processing method. *Radiology*. 2010;257(3):846–853. doi:10.1148/radiol.10100343
65. Bozzali M, Parker GJM, Serra L, et al. Anatomical connectivity mapping: A new tool to assess brain disconnection in Alzheimer's disease. *NeuroImage*. 2011;54(3):2045–2051.
66. Maier-Hein KH, Neher PF, Houde J-C, et al. The challenge of mapping the human connectome based on diffusion tractography. *Nature Communications*. 2017;8(1):1349.
67. Basser PJ, Pierpaoli C. Microstructural and physiological features of tissues elucidated by quantitative-diffusion-tensor MRI. *Journal of Magnetic Resonance, Series B*. 1996;111(3):209–219. doi:10.1006/jmrb.1996.0086
68. Basser PJ, Mattiello J, Lebihan D. MR diffusion tensor spectroscopy and imaging. *Biophysical Journal*. 1994;66:259–267.
69. Raffelt DA, Tournier J-D, Smith RE, et al. Investigating white matter fibre density and morphology using fixel-based analysis. *NeuroImage*. 2017;144:58–73.
70. Raffelt D, Tournier J-D, Rose S, et al. Apparent fibre density: A novel measure for the analysis of diffusion-weighted magnetic resonance images. *NeuroImage*. 2012;59(4):3976–3994.
71. Hagmann P, Cammoun L, Gigandet X, et al. Mapping the structural core of human cerebral cortex. *PLoS Biology*. 2008;6(7):e159.
72. Sherbondy A, Rowe M, Alexander D. MicroTrack: An algorithm for concurrent projectome and microstructure estimation. In: Jiang T, Navab N, Pluim J, Viergever M, eds. *Medical Image Computing and Computer-Assisted Intervention*. Vol 6361. Springer Berlin / Heidelberg; 2010:183–190. https://link.springer.com/chapter/10.1007/978-3-642-15705-9_23
73. Lemkaddem A, Skiöldebrand D, Dal Palú A, Thiran J-P, Daducci A. Global tractography with embedded anatomical priors for quantitative connectivity analysis. *Frontiers in Neurology*. 2014;5:232.
74. Batalle D, Hughes EJ, Zhang H, et al. Early development of structural networks and the impact of prematurity on brain connectivity. *NeuroImage*. 2017;149:379–392. doi:10.1016/j.neuroimage.2017.01.065
75. McColgan P, Seunarine KK, Razi A, et al. Selective vulnerability of Rich Club brain regions is an organizational principle of structural connectivity loss in Huntington's disease. *Brain*. 2015;138(11):3327–3344. doi:10.1093/brain/awv259
76. Proix T, Spiegler A, Schirner M, Rothmeier S, Ritter P, Jirsa VK. How do parcellation size and short-range connectivity affect dynamics in large-scale brain network models? *NeuroImage*. 2016;142:135–149. doi:10.1016/j.neuroimage.2016.06.016
77. Mitra J, Shen K, Ghose S, et al. Statistical machine learning to identify traumatic brain injury (TBI) from structural disconnections of white matter networks. *NeuroImage*. 2016;129:247–259. doi:10.1016/j.neuroimage.2016.01.056
78. McColgan P, Gregory S, Seunarine KK, et al. Brain regions showing white matter loss in Huntington's disease are enriched for synaptic and metabolic genes. *Biological Psychiatry*. 2018;83(5):456–465. doi:10.1016/j.biopsych.2017.10.019
79. Amico E, Goñi J. Mapping hybrid functional-structural connectivity traits in the human connectome. *Network Neuroscience*. 2018;2(3):306–322. doi:10.1162/netn_a_00049
80. Silk TJ, Genc S, Anderson V, et al. Developmental brain trajectories in children with ADHD and controls: A longitudinal neuroimaging study. *BMC Psychiatry*. 2016;16(1):59. doi:10.1186/s12888-016-0770-4
81. Blesa M, Sullivan G, Anblagan D, et al. Early breast milk exposure modifies brain connectivity in preterm infants. *NeuroImage*. 2019;184:431–439. doi:10.1016/j.neuroimage.2018.09.045
82. Takemura H, Pestilli F, Weiner KS, et al. Occipital white matter tracts in human and macaque. *Cerebral Cortex*. 2017;27(6):3346–3359. doi:10.1093/cercor/bhx070
83. Weiner KS, Jonas J, Gomez J, et al. The face-processing network is resilient to focal resection of human visual cortex. *Journal of Neuroscience*. 2016;36(32):8425–8440. doi:10.1523/JNEUROSCI.4509-15.2016
84. Yeatman JD, Weiner KS, Pestilli F, Rokem A, Mezer A, Wandell BA. The vertical occipital fasciculus: A century of controversy resolved by in vivo measurements. *Proceedings of the National Academy of Sciences of the United States of America*. 2014;111(48):E5214–E5223. doi:10.1073/pnas.1418503111
85. Gomez J, Pestilli F, Witthoft N, et al. Functionally defined white matter reveals segregated pathways in human ventral temporal cortex associated with category-specific processing. *Neuron*. 2015;85(1):216–227. doi:10.1016/j.neuron.2014.12.027
86. Takemura H, Rokem A, Winawer J, Yeatman JD, Wandell BA, Pestilli F. A major human white matter pathway between dorsal and ventral visual cortex. *Cerebral Cortex*. 2016;26(5):2205–2214. doi:10.1093/cercor/bhv064
87. Ajina S, Pestilli F, Rokem A, Kennard C, Bridge H. Human blindsight is mediated by an intact geniculo-extrastriate pathway. *eLife*. 2015;4:e08935. doi:10.7554/eLife.08935
88. Perge JA, Niven JE, Mugnaini E, Balasubramanian V, Sterling P. Why do axons differ in caliber? *The Journal of Neuroscience: The Official Journal of the Society for Neuroscience*. 2012;32(2):626–638.
89. Drobnjak I, Zhang H, Ianuş A, Kaden E, Alexander DC. PGSE, OGSE, and sensitivity to axon diameter in diffusion MRI: Insight from a simulation study. *Magnetic Resonance in Medicine*. 2016;75(2):688–700. doi:10.1002/mrm.25631
90. Whittall KP, Mackay AL, Graeb DA, Nugent RA, Li DKB, Paty DW. In vivo measurement of T2 distributions and water contents in normal human brain. *Magnetic Resonance in Medicine*. 1997;37(1):34–43. doi:10.1002/mrm.1910370107
91. Fan Q, Nummenmaa A, Witzel T, et al. Axon diameter index estimation independent of fiber orientation distribution using high-gradient diffusion MRI. *NeuroImage*. 2020;222:117197. doi:10.1016/j.neuroimage.2020.117197

92. Zhang H, Hubbard PL, Parker GJM, Alexander DC. Axon diameter mapping in the presence of orientation dispersion with diffusion MRI. *NeuroImage*. 2011;56(3):1301–1315.
93. Veraart J, Nunes D, Rudrapatna U, et al. Nonivasive quantification of axon radii using diffusion MRI. *eLife*. 2020;9:e49855. doi:10.7554/eLife.49855
94. Beaulieu C. The basis of anisotropic water diffusion in the nervous system – a technical review. *NMR in Biomedicine*. 2002;15(7–8):435–455.
95. Swadlow H, Waxman S. Axonal conduction delays. *Scholarpedia*. 2012;7:1451.
96. Yeh C-H, Smith RE, Dhollander T, Calamante F, Connelly A. Connectomes from streamlines tractography: Assigning streamlines to brain parcellations is not trivial but highly consequential. *NeuroImage*. 2019;199:160–171. doi:10.1016/j.neuroimage.2019.05.005
97. Yeh C-H, Smith RE, Dhollander T, Connelly A. Mesh-based anatomically-constrained tractography for effective tracking termination and structural connectome construction. *Proceedings of the ISMRM*. 2017:0058. https://www.researchgate.net/publication/315836374_Mesh-based_anatomically-constrained_tractography_for_effective_tracking_termination_and_structural_connectome_construction
98. Smith R, Skoch A, Bajada C, Caspers S, Connelly A. Hybrid surface-volume segmentation for improved anatomically-constrained tractography. In: *Organisation for Human Brain Mapping*. 2020:1034. https://www.researchgate.net/publication/342800028_Hybrid_Surface-Volume_Segmentation_for_improved_Anatomically-Constrained_Tractography
99. Morris DM, Embleton KV, Parker GJM. Probabilistic fibre tracking: Differentiation of connections from chance events. *NeuroImage*. 2008;42(4):1329–1339.
100. Tournier J-D, Smith R, Raffelt D, et al. MRtrix3: A fast, flexible and open software framework for medical image processing and visualisation. *NeuroImage*. 2019;202:116137. doi:10.1016/j.neuroimage.2019.116137

Appendix

Algorithm 1: 'Fixel mask'

```
define pathway.fixels = empty_set
define pathway.volume = 0.0
for s in pathway.streamlines:
  for f in s.fixels_traversed:
    if f not in pathway.fixels:
      pathway.fixels += f
      pathway.volume += f.volume
    end if
  end for
end for
define pathway.sum_lengths = 0.0
for s in pathway.streamlines:
  pathway.sum_lengths += s.length
end for
define pathway.mean_length = pathway.sum_lengths / pathway.number_of_streamlines
define pathway.connectivity = pathway.volume / pathway.mean_length
```

Algorithm 2: 'Weighted fixel mask'

```
for s in tractogram.streamlines:
  for f in s.fixels_traversed:
    f.tractogram_density += s.length_within_fixel[f]
    if s in pathway.streamlines:
      f.pathway_density += s.length_within_fixel[f]
  end for
end for
define pathway.volume = 0.0
for f in fixels:
  pathway.volume += (f.volume * f.pathway_density / f.tractogram_density)
end for
define pathway.sum_lengths = 0.0
for s in pathway.streamlines:
  pathway.sum_lengths += s.length
end for
define pathway.mean_length = pathway.sum_lengths / pathway.number_of_streamlines
define pathway.connectivity = pathway.volume / pathway.mean_length
```

Algorithm 3: 'Volume-averaged streamlines weights'

```
for s in tractogram.streamlines:
  for f in fixels_traversed_by_s:
    f.tractogram_density += s.length_within_fixel[f]
  end for
end for
define pathway.connectivity = 0.0
for s in pathway.streamlines:
  define s.volume = 0.0
  for f in fixels_traversed_by_s:
    s.volume += (f.volume * s.length_within_fixel[f] / f.tractogram_density)
  end for
  define s.crosssection = s.volume / s.length
  pathway.connectivity += s.crosssection
end for
```


Algorithm 4: 'Optimized streamlines weights'

```
define error = sum (f.density - f.tractogram_density)^2 for all fixels "f"
for i in iterations:
  for s in tractogram.streamlines:
    optimize s.crosssection to minimise error
  end for
end for
define pathway.connectivity = 0.0
for s in pathway.streamlines:
  add s.crosssection to pathway.connectivity
end for
```

